# Tracking Detector Development for the International Linear Collider

CP3 SEMINAR

**PAUL MALEK**

14 MAY 2024

Introduction to ILC

Overview of ILD

TPC Development for ILD

# Future $e^+e^-$ Colliders

- discovery of 125 GeV Higgs boson by ATLAS & CMS in 2021
- consensus for "Higgs Factory" as next big project in particle physics
  - LHC cannot fully determine Higgs properties
  - Higgs boson as window into BSM physics
- several concepts
  - circular: FCC-ee, CEPC
  - linear: CLIC, ILC
- $e^+e^-$ collider with $E_{\mathrm{cm}} \geq 250$ GeV
  - Higgs-strahlung peak ($e^+e^- \to ZH$)
- further energy POIs:
  - $t\bar{t}$ threshold (350 GeV)
  - $t\bar{t}H$ / $ZHH$ ($\geq$ 500 GeV)

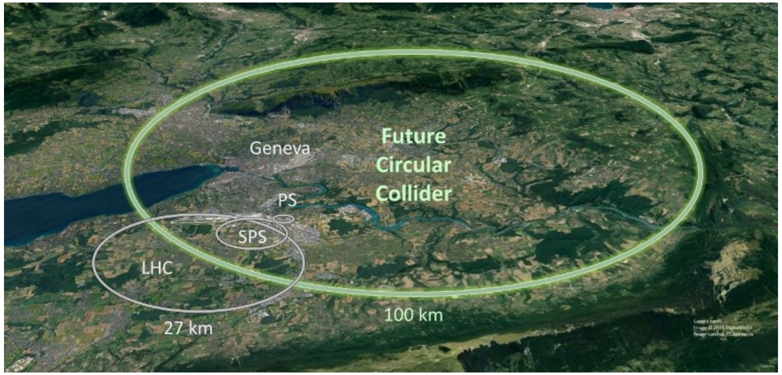


# Future $e^+e^-$ Colliders

- discovery of 125 GeV Higgs boson by ATLAS & CMS in 2021
- consensus for “Higgs Factory” as next big project in particle physics
  - LHC cannot fully determine Higgs properties
  - Higgs boson as window into BSM physics
- several concepts
  - circular: FCC-ee, CEPC
  - linear: CLIC, ILC
- $e^+e^-$ collider with $E_{cm} \geq 250$ GeV
  - Higgs-strahlung peak ($e^+e^- \to ZH$)
- further energy POIs:
  - $t\bar{t}$ threshold (350 GeV)
  - $t\bar{t}H$ / $ZHH$ ($\geq$ 500 GeV)

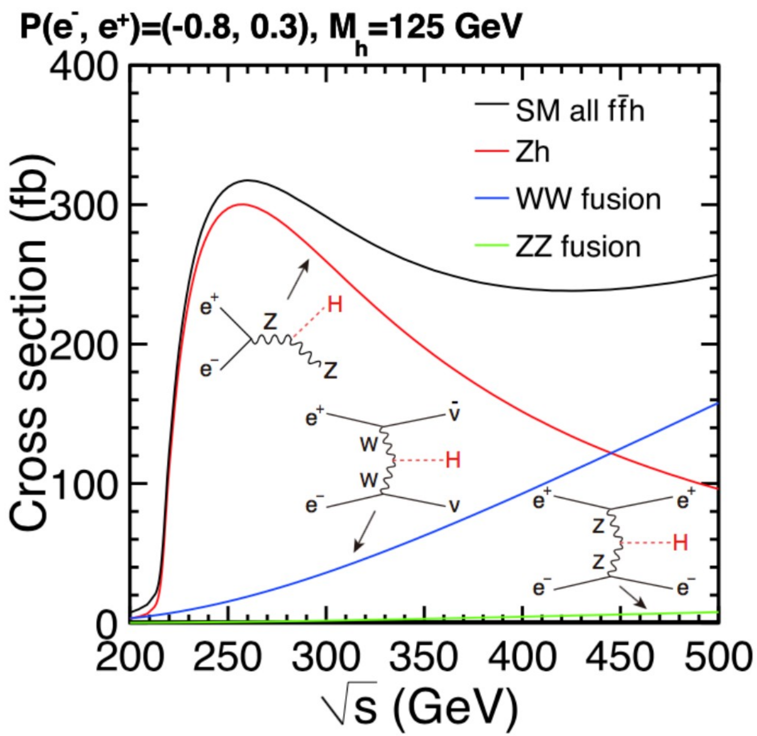

# The International Linear Collider

- accelerator design result of ~20y of R&D
- candidate site in the Kitakami area, Japan
  - suitable for up to 50 km tunnel
- 20 km baseline design with $E_{CM}$ = 250 GeV
  - upgradable to 500 GeV (30 km)
- accelerator based on 1.3 GHz SCRF cavities
  - design gradient: 31.5 MV/m - 35 MV/m
  - proven technology: E-XFEL, LCLS-II
- design luminosity of $1.35 \times 10^{34}$ $cm^{-2}s^{-1}$
  - double with luminosity upgrade
- 1312 (2625) bunches in ~1 ms long pulses
  - 5 Hz repetition rate
- 80% electron polarisation, (30% positrons)
- 2 detectors in “push-pull” configuration

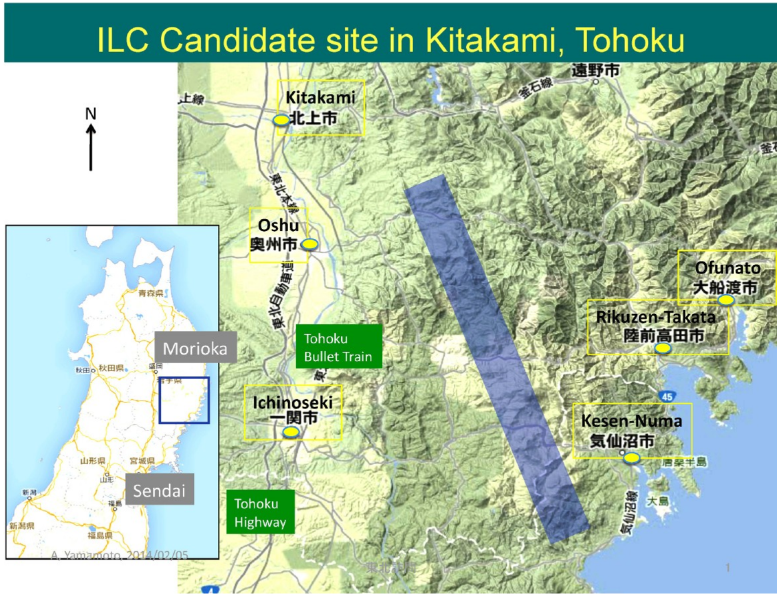

# The International Linear Collider

- accelerator design result of ~20y of R&D
- candidate site in the Kitakami area, Japan
  - suitable for up to 50 km tunnel
- 20 km baseline design with $E_{CM}$ = 250 GeV
  - upgradable to 500 GeV (30 km)
- accelerator based on 1.3 GHz SCRF cavities
  - design gradient: 31.5 MV/m - 35 MV/m
  - proven technology: E-XFEL, LCLS-II
- design luminosity of $1.35 \times 10^{34}$ $cm^{-2}s^{-1}$
  - double with luminosity upgrade
- 1312 (2625) bunches in ~1 ms long pulses
  - 5 Hz repetition rate
- 80% electron polarisation, (30% positrons)
- 2 detectors in “push-pull” configuration

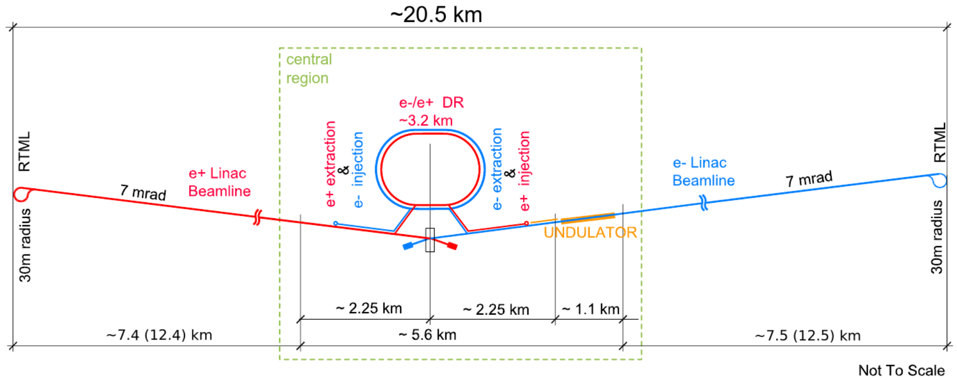


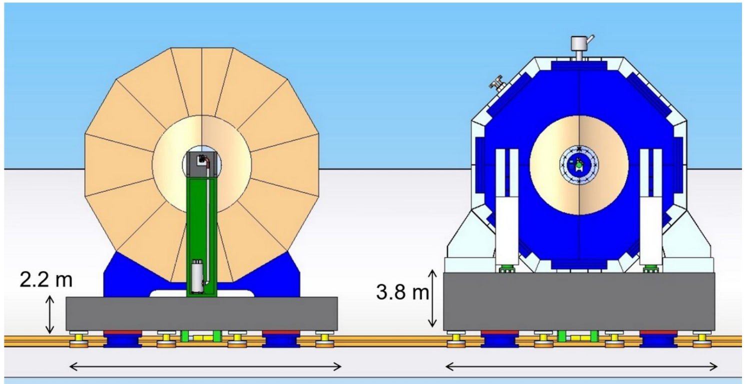

# Physics at the ILC

**at 250 GeV (2 ab$^{-1}$):**

- improve Higgs mass precision to 14 MeV
  - recoil-mass technique
- directly measure total width of the Higgs
- measure Higgs couplings to < 1%
  - gauge bosons, 3rd gen. fermions
  - BSM deviations expected at ~5%
- limit invisible Higgs decay width to < 0.16%
- measurement of $m_W$ to 2.5 MeV
- triple gauge couplings to O($10^{-3}$)

**at higher energies:**

- Higgs self coupling to < 30%
- top quark mass to 20 MeV

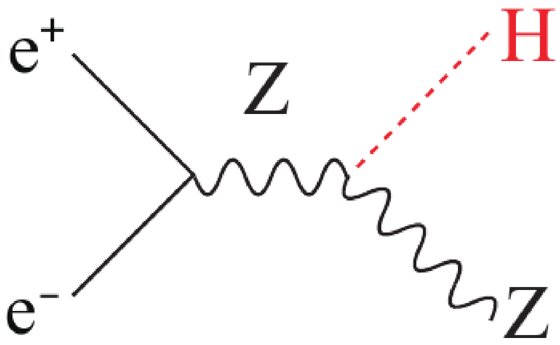


arXiv:1306.6329 [physics.ins-det]

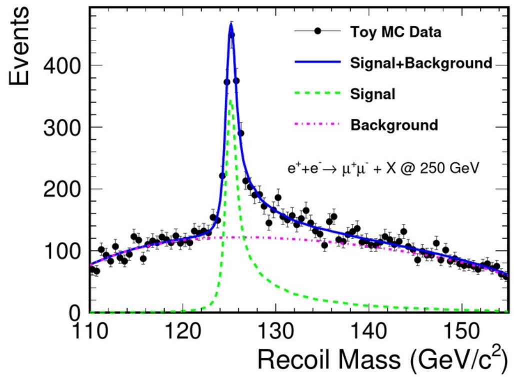


arXiv:2203.07622 [physics.acc-ph]

# Physics at the ILC

**at 250 GeV (2 $ab^{-1}$):**

- improve Higgs mass precision to 14 MeV
  - recoil-mass technique
- directly measure total width of the Higgs
- measure Higgs couplings to < 1%
  - gauge bosons, 3rd gen. fermions
  - BSM deviations expected at ~5%
- limit invisible Higgs decay width to < 0.16%
- measurement of $m_W$ to 2.5 MeV
- triple gauge couplings to $O(10^{-3})$

**at higher energies:**

- Higgs self coupling to < 30%
- top quark mass to 20 MeV

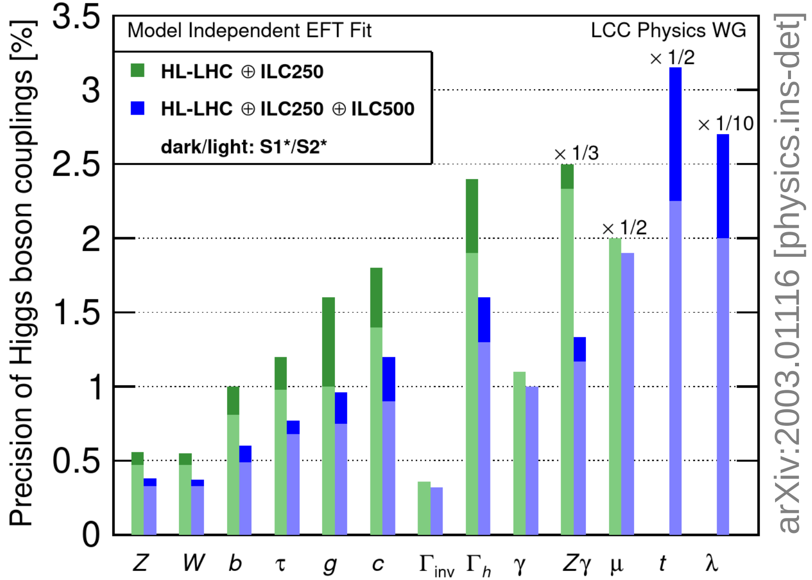

# The International Large Detector

- general-purpose 4π particle detector for ILC
- detector specifications driven by physics requirements
  - Higgs recoil mass → momentum resolution
    - $\Delta(1/p_T) = \frac{\Delta p_T}{p_T^2} \leq 2 \cdot 10^{-5}\,\text{GeV}^{-1} \oplus \frac{10^{-3}}{p_T \sin\theta}$
  - Higgs BR to $b/c/\tau$ → vertex resolution
    - $\sigma_{d_0} \leq 5\,\mu\text{m} \oplus \frac{10\,\mu\text{m}}{(p/\text{GeV})(\sin\theta)^{3/2}}$
  - $W/Z$ dijet mass separation → jet energy resolution
    - $\Delta E/E \approx 3\%$ for $E \geq 100$ GeV

→ optimized for particle flow
  - highly granular calorimeters inside a 3.5 T solenoid
  - highly efficient tracking system: TPC + silicon
    - > 99% efficiency for $p_T > 250$ MeV
  - minimal material in inner detector
    - barrel: ~0.1 $X_0$; endcaps: ~0.5 $X_0$

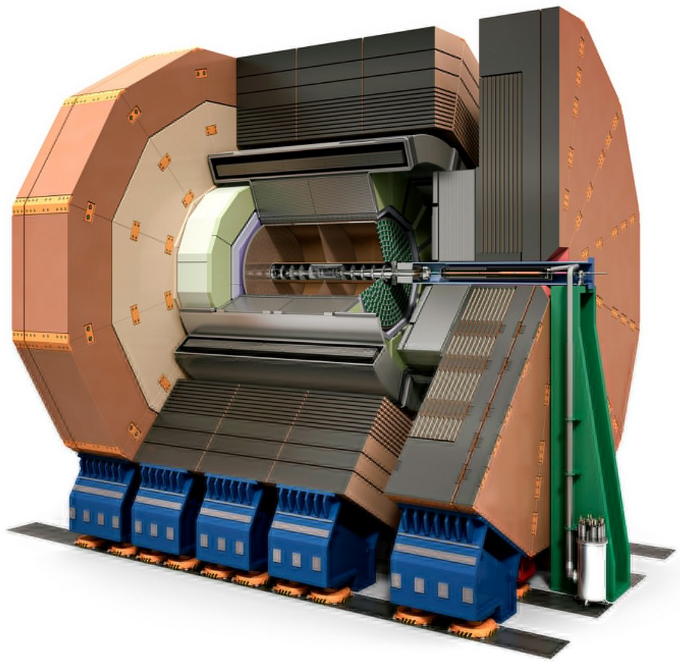

# The International Large Detector

- general-purpose 4π particle detector for ILC
- detector specifications driven by physics requirements
  - Higgs recoil mass → momentum resolution
    - $\Delta(1/p_T) = \frac{\Delta p_T}{p_T^2} \leq 2\cdot10^{-5}\,\mathrm{GeV}^{-1} \oplus \frac{10^{-3}}{p_T \sin\theta}$ ≈ CMS/10 ALEPH/30
  - Higgs BR to $b/c/\tau$ → vertex resolution
    - $\sigma_{d_0} \leq 5\,\mu\mathrm{m} \oplus \frac{10\,\mu\mathrm{m}}{(p/\mathrm{GeV})(\sin\theta)^{3/2}}$ ≤ CMS/2 | ALEPH/2
  - $W/Z$ dijet mass separation → jet energy resolution
    - $\Delta E/E \approx 3\%$ for $E \geq 100$ GeV ≈ CMS/3

→ optimized for particle flow
  - highly granular calorimeters inside a 3.5 T solenoid
  - highly efficient tracking system: TPC + silicon
    - > 99% efficiency for $p_T > 250$ MeV
  - minimal material in inner detector
    - barrel: ~0.1 $X_0$; endcaps: ~0.5 $X_0$ ≈ CMS/2

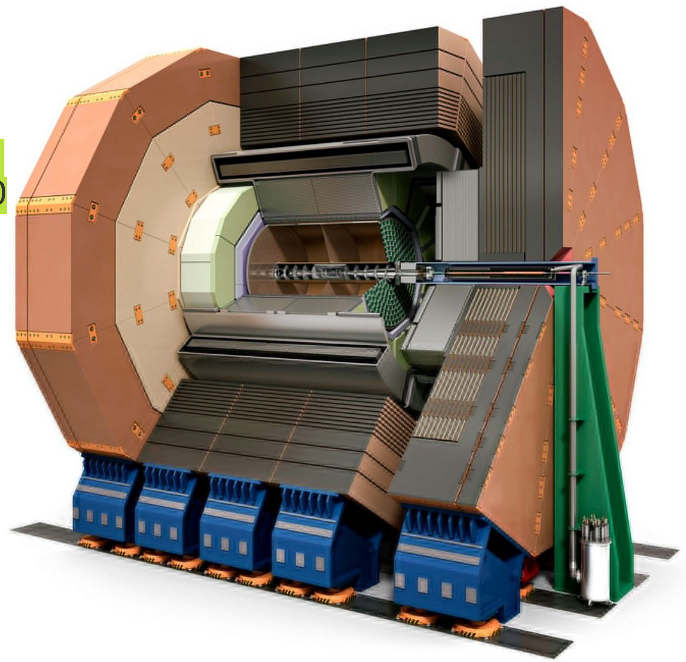

# Particle Flow

- precision of jet energy measurement limited by HCAL resolution
- combine information from all subdetectors to improve jet energy resolution
  - 65% charged particles → tracker momentum
  - 25% photons → ECAL energy measurement
    - $\Delta E/E \leq 20\%/\sqrt{E/\mathrm{GeV}}$
  - 10% neutral hadrons → HCAL energy
    - $\Delta E/E \geq 50\%/\sqrt{E/\mathrm{GeV}}$
- separate individual particle contributions & match tracks and calorimeter showers
  → major driver for calorimeter & tracker design
    - e.g. tungsten ECAL: large ratio $\lambda/X_0$
- precision limited by wrong shower separation
  → "confusion"
  - more prevalent at higher energies

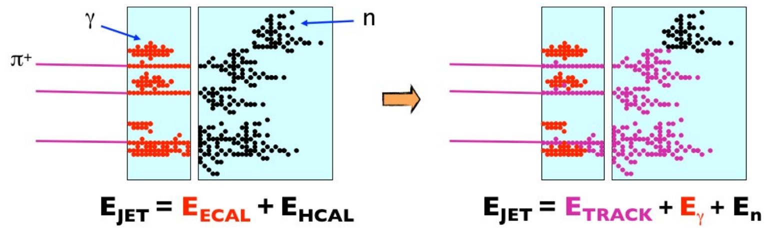


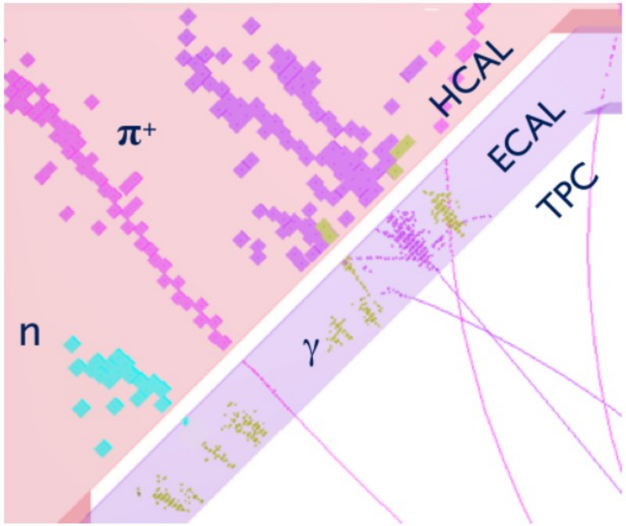


arXiv:1308.4537 [physics.ins-det]

# Particle Flow

- precision of jet energy measurement limited by HCAL resolution
- combine information from all subdetectors to improve jet energy resolution
  - 65% charged particles → tracker momentum
  - 25% photons → ECAL energy measurement
    - $\Delta E/E \leq 20\%/\sqrt{E/\text{GeV}}$
  - 10% neutral hadrons → HCAL energy
    - $\Delta E/E \geq 50\%/\sqrt{E/\text{GeV}}$
- separate individual particle contributions & match tracks and calorimeter showers
  → major driver for calorimeter & tracker design
    - e.g. tungsten ECAL: large ratio $\lambda/X_0$
- precision limited by wrong shower separation
  → "confusion"
  - more prevalent at higher energies

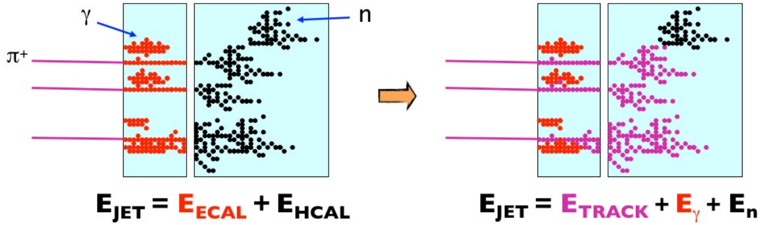


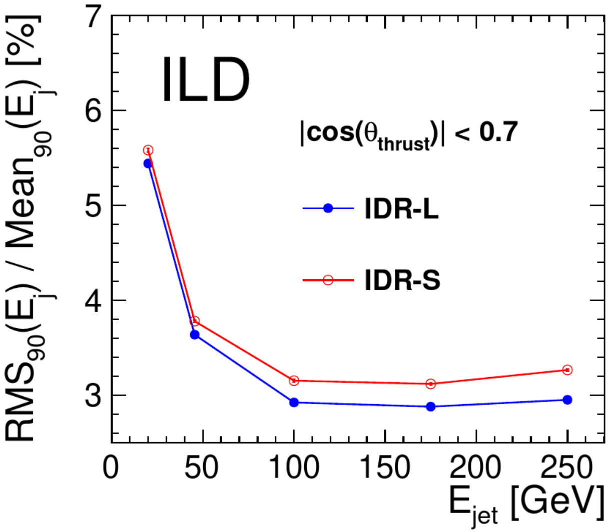


arXiv:2003.01116 [physics.ins-det]

# Particle Flow

- precision of jet energy measurement limited by HCAL resolution
- combine information from all subdetectors to improve jet energy resolution
  - 65% charged particles → tracker momentum
  - 25% photons → ECAL energy measurement
    - $\Delta E / E \leq 20\% / \sqrt{E/\mathrm{GeV}}$
  - 10% neutral hadrons → HCAL energy
    - $\Delta E / E \geq 50\% / \sqrt{E/\mathrm{GeV}}$
- separate individual particle contributions & match tracks and calorimeter showers
  → major driver for calorimeter & tracker design
    - e.g. tungsten ECAL: large ratio $\lambda/X_0$
- precision limited by wrong shower separation
  → "confusion"
  - more prevalent at higher energies

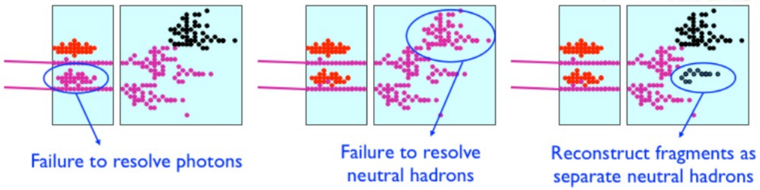


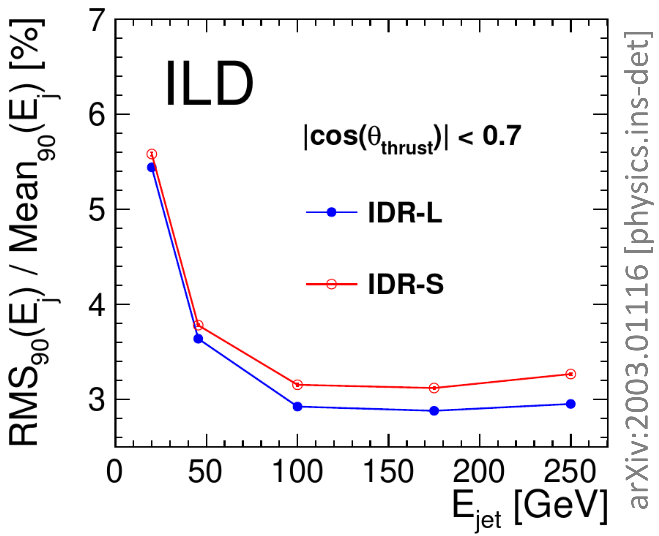

# The International Large Detector

- general-purpose 4π particle detector for ILC
- detector specifications driven by physics requirements
  - Higgs recoil mass → momentum resolution
    - $\Delta(1/p_T) = \frac{\Delta p_T}{p_T^2} \leq 2 \cdot 10^{-5}\,\mathrm{GeV}^{-1} \oplus \frac{10^{-3}}{p_T \sin\theta}$ ≈ CMS/10 ALEPH/30
  - Higgs BR to $b/c/\tau$ → vertex resolution
    - $\sigma_{d_0} \leq 5\,\mu\mathrm{m} \oplus \frac{10\,\mu\mathrm{m}}{(p/\mathrm{GeV})(\sin\theta)^{3/2}}$ ≤ CMS/2 | ALEPH/2
  - $W/Z$ dijet mass separation → jet energy resolution
    - $\Delta E/E \approx 3\%$ for $E \geq 100$ GeV ≈ CMS/3

→ optimized for particle flow
  - highly granular calorimeters inside a 3.5 T solenoid
  - highly efficient tracking system: TPC + silicon
    - > 99% efficiency for $p_T > 250$ MeV
  - minimal material in inner detector
    - barrel: ~0.1 $X_0$; endcaps: ~0.5 $X_0$ ≈ CMS/2

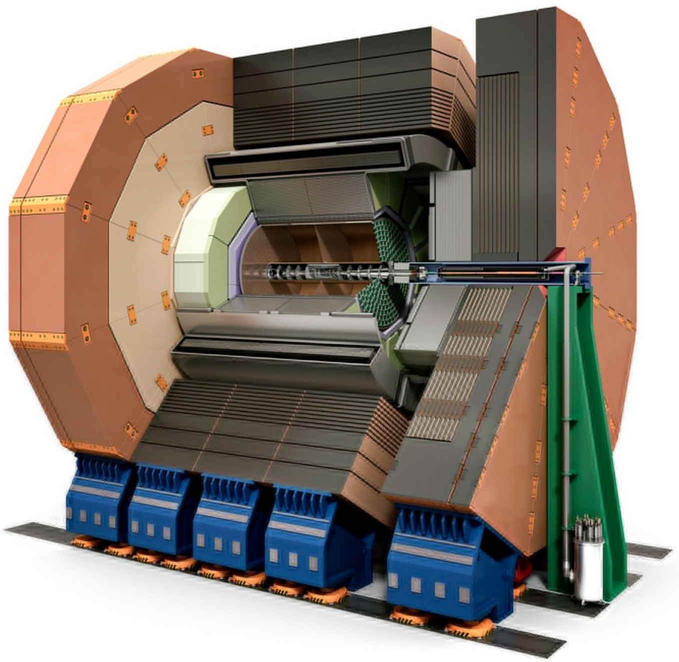

# ILD Event Display

$e^+e^- \rightarrow t\bar{t}H \rightarrow 6qb\bar{b}$

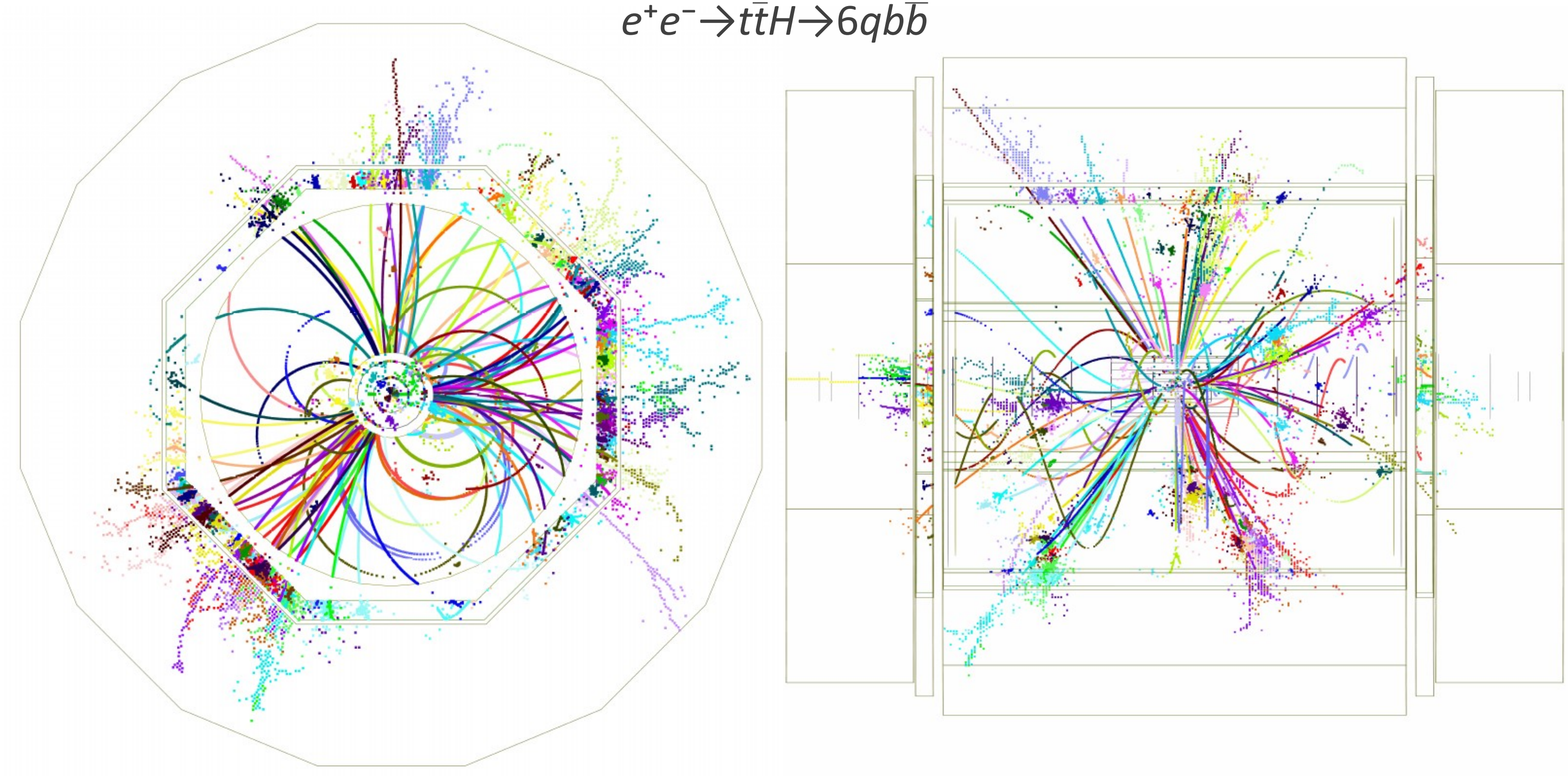

arXiv:1306.6329 [physics.ins-det]

# ILD Sub-detectors

- vertex detector: 3 double-layers silicon pixel sensors
  - material ≤ 0.15% $X_0$ per layer
  - spatial resolution = 3 µm
- inner silicon tracker: 2 double layers pixel sensors
  - spatial resolution = 5 µm
- forward tracker: 2 pixel + 5 stereo strip layers
  - extends tracking coverage to θ = 4.8°
- Time Projection Chamber
- outer silicon layer: 1 stereo layer strip sensors
  - transverse resolution = 7 µm
  - considered as timing layer for TOF (10 ps)
- ECAL: 30 layers tungsten + silicon / scintillator
  - depth of 24 $X_0$ / 0.85 λ
  - 5 mm cell size
- HCAL: 48 layers steel + scintillator / RPC
  - depth of 6 λ
  - 3 cm / 1cm cell size

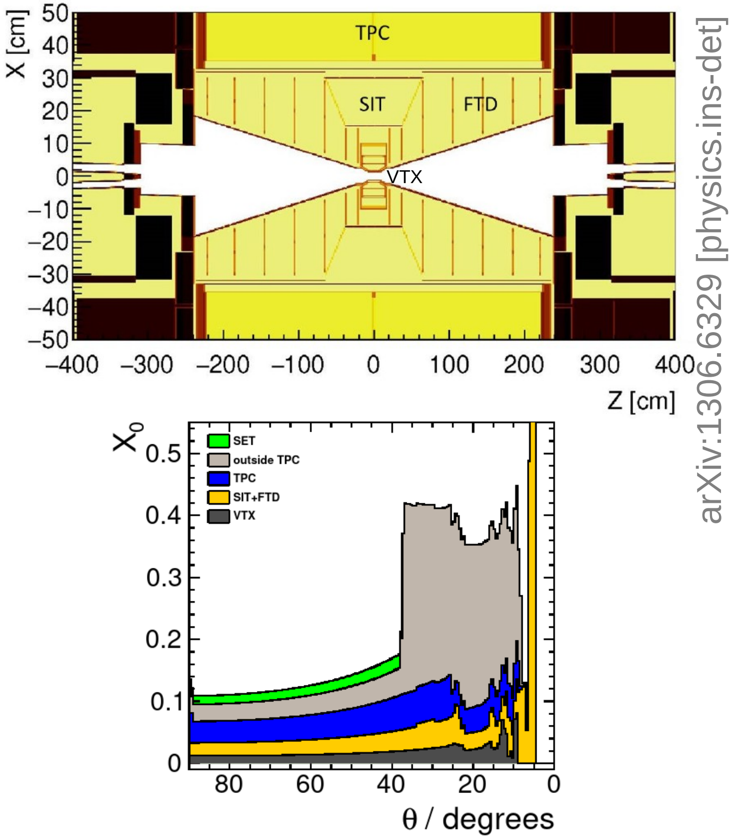

# ILD Sub-detectors

- vertex detector: 3 double-layers silicon pixel sensors
  - material ≤ 0.15% $X_0$ per layer
  - spatial resolution = 3 µm
- inner silicon tracker: 2 double layers pixel sensor
  - spatial resolution = 5 µm
- forward tracker: 2 pixel + 5 stereo strip layers
  - extends tracking coverage to θ = 4.8°
- Time Projection Chamber
- outer silicon layer: 1 stereo layer strip sensors
  - transverse resolution = 7 µm
  - considered as timing layer for TOF (10 ps)
- ECAL: 30 layers tungsten + silicon / scintillator
  - depth of 24 $X_0$ / 0.85 λ
  - 5 mm cell size
- HCAL: 48 layers steel + scintillator / RPC
  - depth of 6 λ
  - 3 cm / 1cm cell size

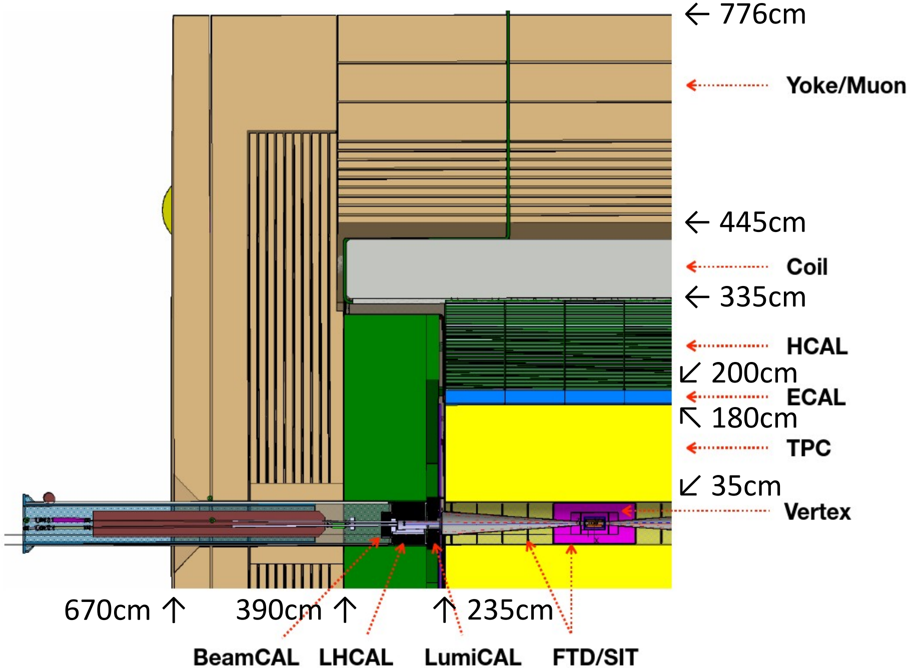


arXiv:1306.6329 [physics.ins-det]

# The ILD Time Projection Chamber

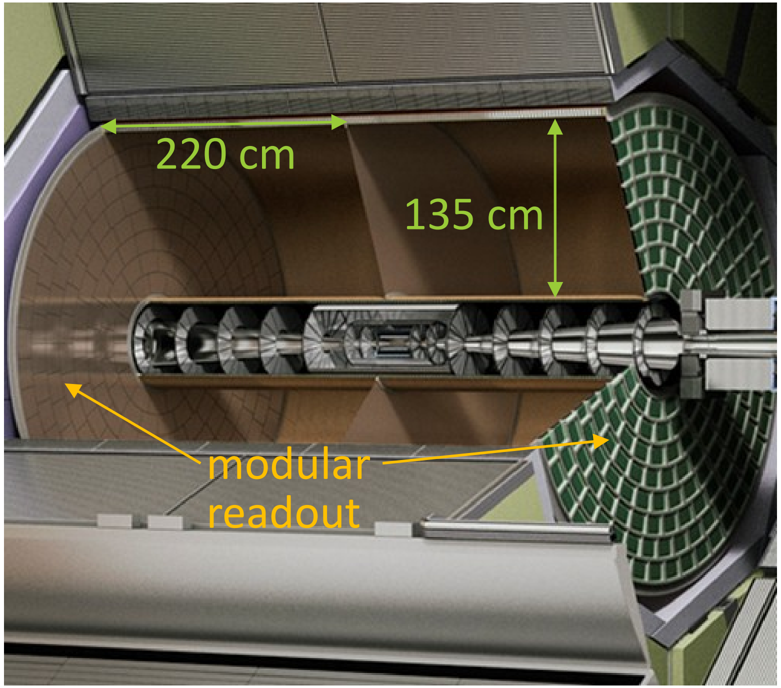


- field cage ~5% $X_0$; end caps < 25% $X_0$
  ≈ ALICE
- TPC standalone resolution requirement
  - $\Delta p_T / p_T \leq 10^{-4} (p_T/\text{GeV}) \Rightarrow \sigma_{r\varphi} \leq 100\,\mu\text{m}$
    ≈ ALEPH/12 ≈ ALEPH/2
- gas amplification by MPGD:
  - GEM or MicroMEGAS
  - small readout electrodes: ~1 mm × 6 mm
  - alternative: GridPix (55 µm pixels)
- 220 samples per track for 35 cm < r < 170 cm
  - high redundancy / efficiency
  - excellent pattern recognition capabilities
  - ↳ matching of tracks and calorimeter clusters
- specific energy loss measurement for PID
  - expected dE/dx resolution: ~5% ≈ ALEPH | ALICE

# The ILD Time Projection Chamber

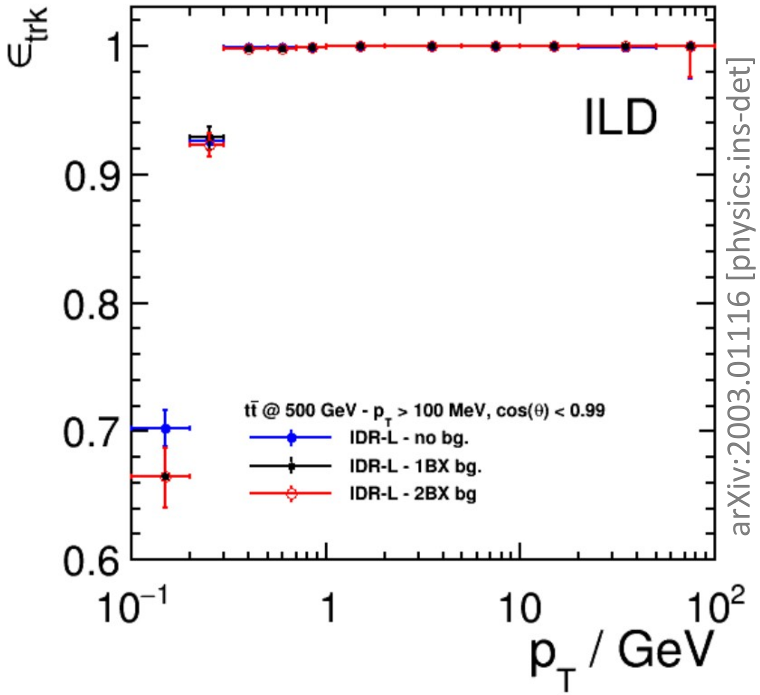


arXiv:2003.01116 [physics.ins-det]

- field cage ~5% $X_0$; end caps < 25% $X_0$ ≈ ALICE
- TPC standalone resolution requirement
  - $\Delta p_T / p_T \leq 10^{-4} (p_T/\text{GeV}) \Rightarrow \sigma_{r\varphi} \leq 100\,\mu\text{m}$ (≈ ALEPH/12; ≈ ALEPH/2)
- gas amplification by MPGD:
  - GEM or MicroMEGAS
  - small readout electrodes: ~1 mm × 6 mm
  - alternative: GridPix (55 µm pixels)
- 220 samples per track for 35 cm < r < 170 cm
  - high redundancy / efficiency
  - excellent pattern recognition capabilities
  - ↳ matching of tracks and calorimeter clusters
- specific energy loss measurement for PID
  - expected dE/dx resolution: ~5% ≈ ALEPH | ALICE

# Time Projection Chambers

- gas filled volume with (homogeneous) electric field
- fast charged incident particles ionise gas long their path
  - electric field separates electron-ion pairs
- electrons drift to the anode
  - magnetic field parallel to electric field reduces diffusion
- track “image” is projected onto segmented readout
  - avalanche gas amplification required
- 3rd coordinate reconstructed from arrival time and drift velocity

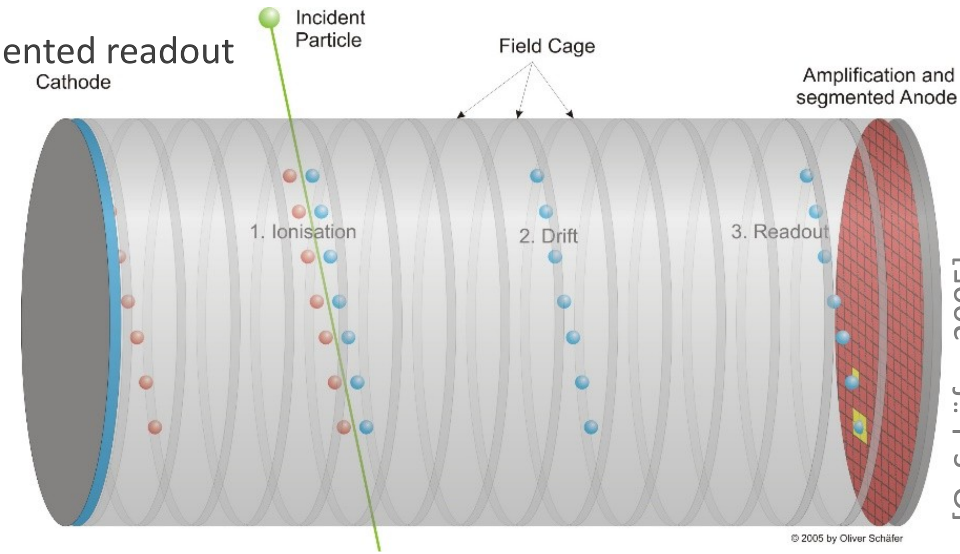


[O. Schäfer, 2005]

# Gas Electron Multipliers

- insulating foil coated with copper on both sides
  - holes allow transfer of electrons
- high voltage between electrodes creates strong field in holes (> 10 kV/cm)
  → avalanche gas amplification
- external fields influence GEM transparency for electrons and ions
  - field dependency for electrons and ions generally inverted
  → fields can be tuned to absorb ions
  → reduces space charge induced field distortions

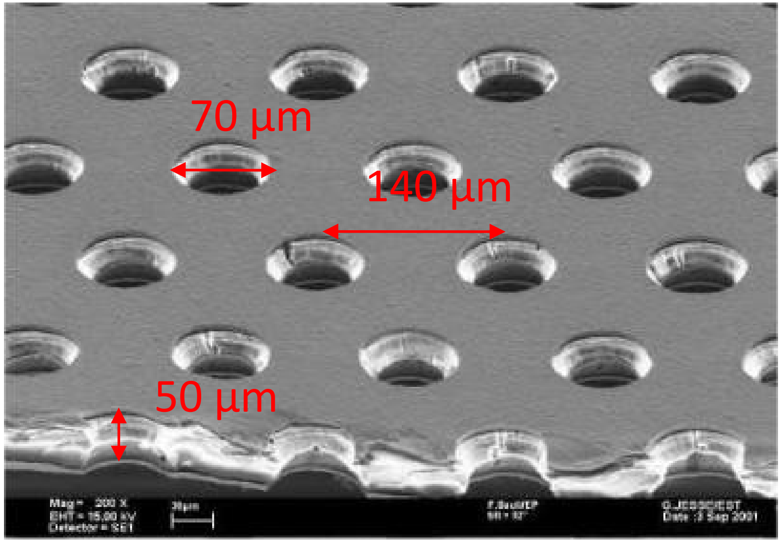


[CERN GDD]

# Gas Electron Multipliers

- insulating foil coated with copper on both sides
  - holes allow transfer of electrons
- high voltage between electrodes creates strong field in holes (> 10 kV/cm)
  → avalanche gas amplification
- external fields influence GEM transparency for electrons and ions
  - field dependency for electrons and ions generally inverted
  → fields can be tuned to absorb ions
  → reduces space charge induced field distortions

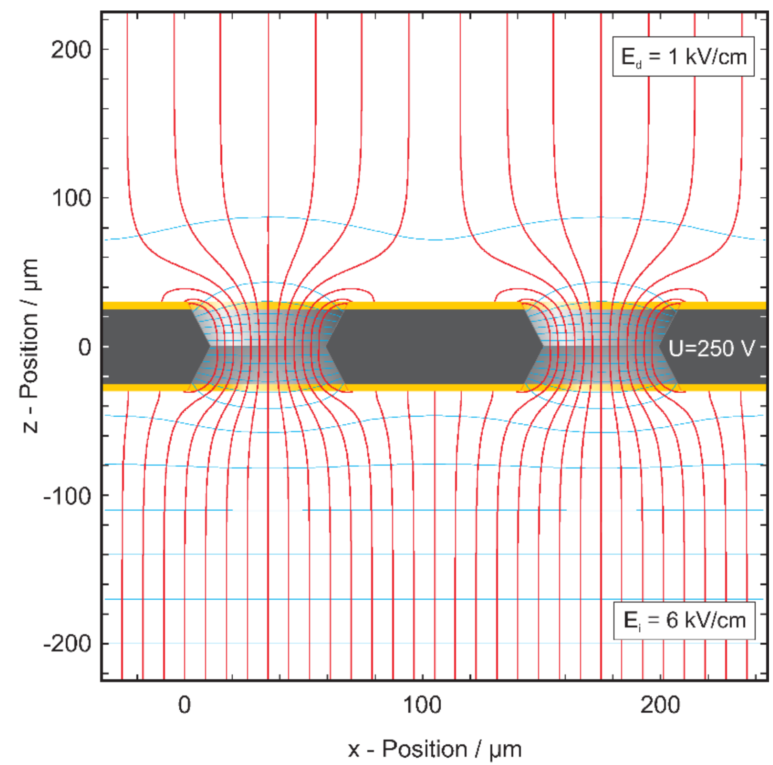


[O. Schäfer, 2006]

# Gas Electron Multipliers

- insulating foil coated with copper on both sides
  - holes allow transfer of electrons
- high voltage between electrodes creates strong field in holes (> 10 kV/cm)
  → avalanche gas amplification
- external fields influence GEM transparency for electrons and ions
  - field dependency for electrons and ions generally inverted
  → fields can be tuned to absorb ions
  → reduces space charge induced field distortions

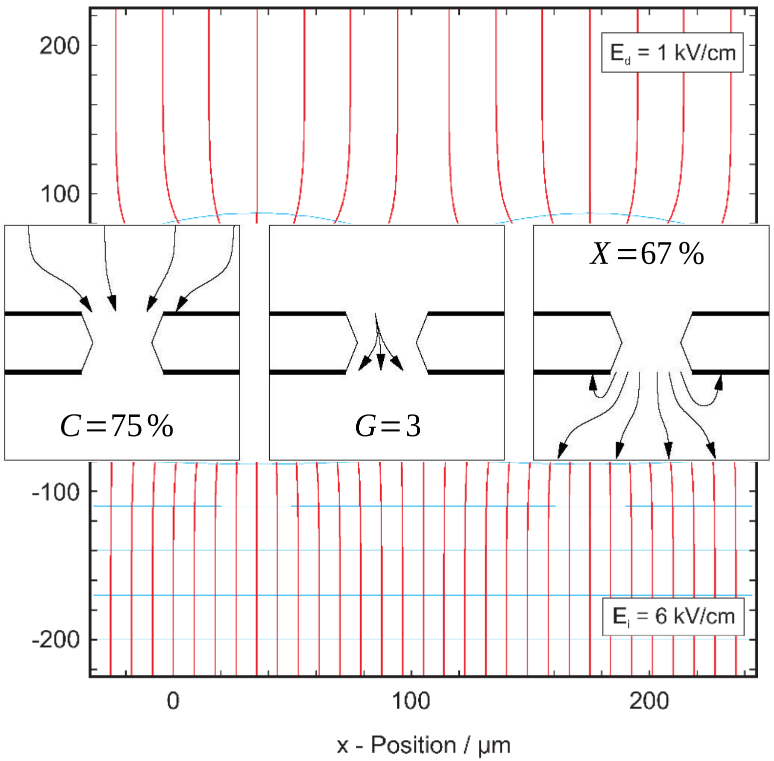

# The GridGEM Readout Module

- aluminium back frame
  - provides rigidity & mounting points
- passive readout board w/ segmented anode
  - 28 rows, 4828 pads
- stack of 3 GEMs
  - mounted on thin ceramic frames
  - ~95% active area

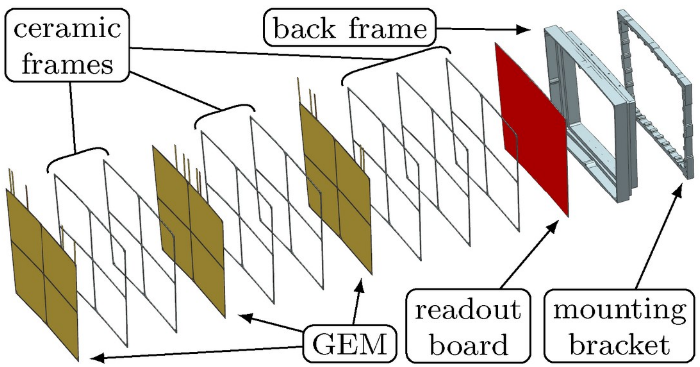


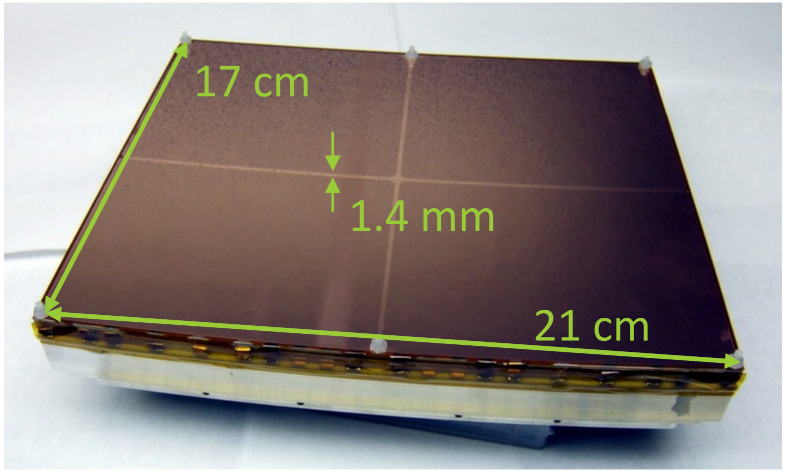

# The GridGEM Readout Module

- aluminium back frame
  - provides rigidity & mounting points
- passive readout board w/ segmented anode
  - 28 rows, 4828 pads
- stack of 3 GEMs
  - mounted on thin ceramic frames
  - ~95% active area

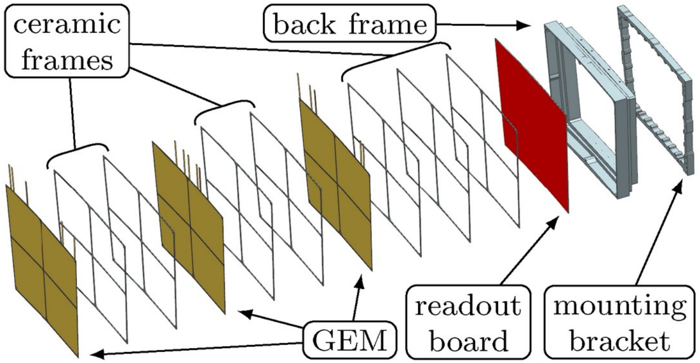


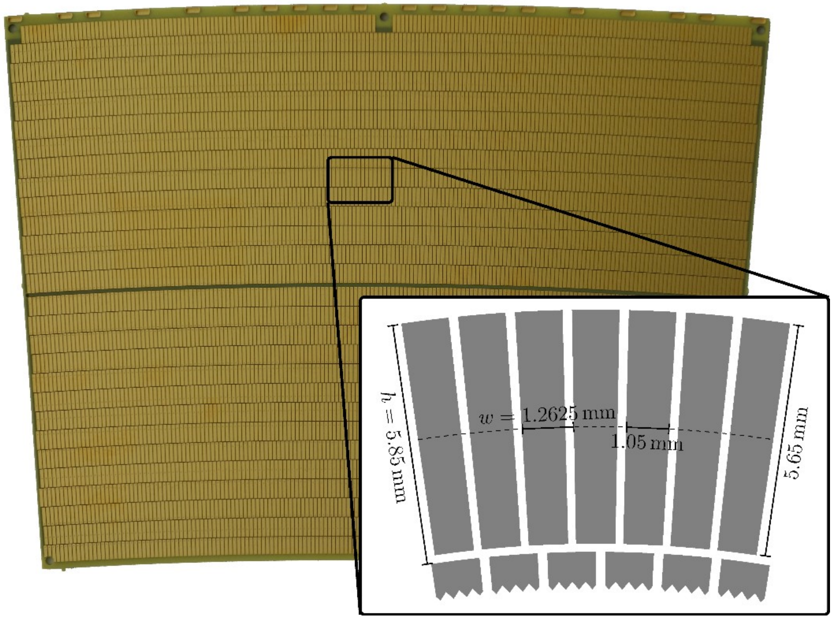

# The GridGEM Readout Module

- aluminium back frame
  - provides rigidity & mounting points
- passive readout board w/ segmented anode
  - 28 rows, 4828 pads
- stack of 3 GEMs
  - mounted on thin ceramic frames
  - ~95% active area

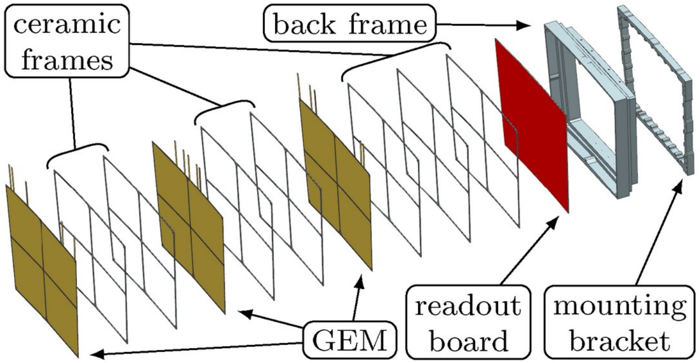


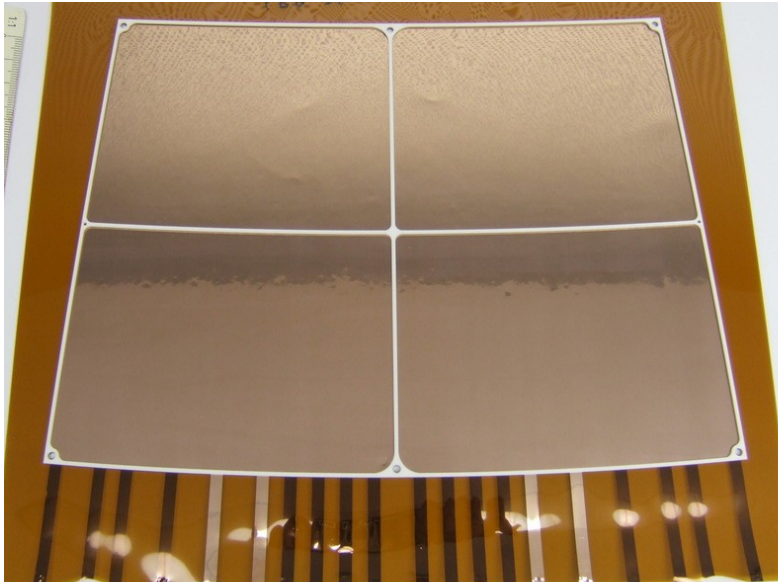

# The GridGEM Readout Module

- aluminium back frame
  - provides rigidity & mounting points
- passive readout board w/ segmented anode
  - 28 rows, 4828 pads
- stack of 3 GEMs
  - mounted on thin ceramic frames
  - ~95% active area

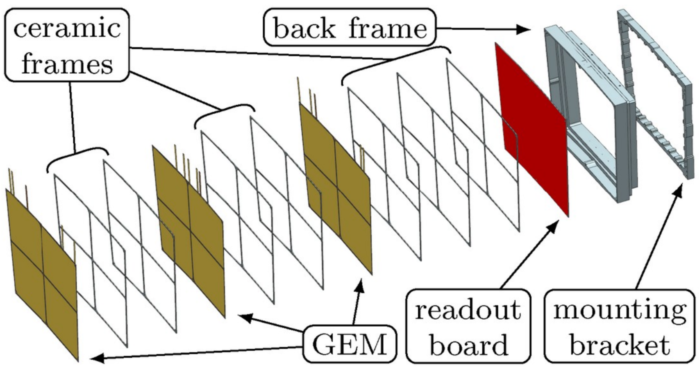


# The Importance of Flat GEMs

- GEM deflections affect field homogeneity
- drift field distortions introduce E×B effects
  - can deteriorate spatial resolution
- inter-GEM fields influence GEM transparency for electrons
- non-uniformity introduces variations of effective gain

→ minimise deflection to not affect momentum & dE/dx measurement

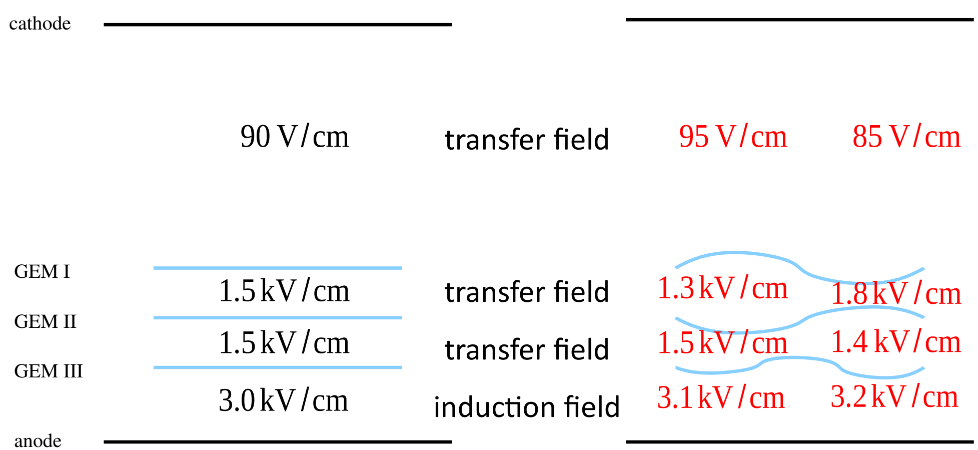


doi: 10.3204/DESY-THESIS-2010-015

# The Importance of Flat GEMs

- GEM deflections affect field homogeneity
- drift field distortions introduce E×B effects
  - can deteriorate spatial resolution
- inter-GEM fields influence GEM transparency for electrons
- non-uniformity introduces variations of effective gain

→ minimise deflection to not affect momentum & dE/dx measurement

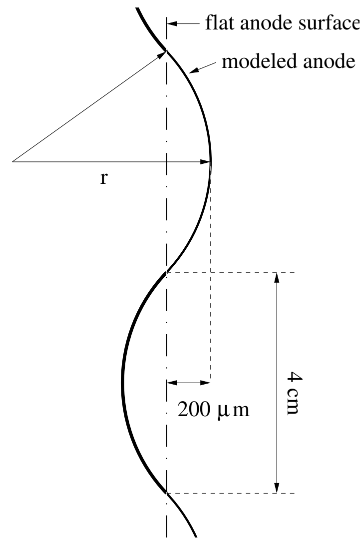


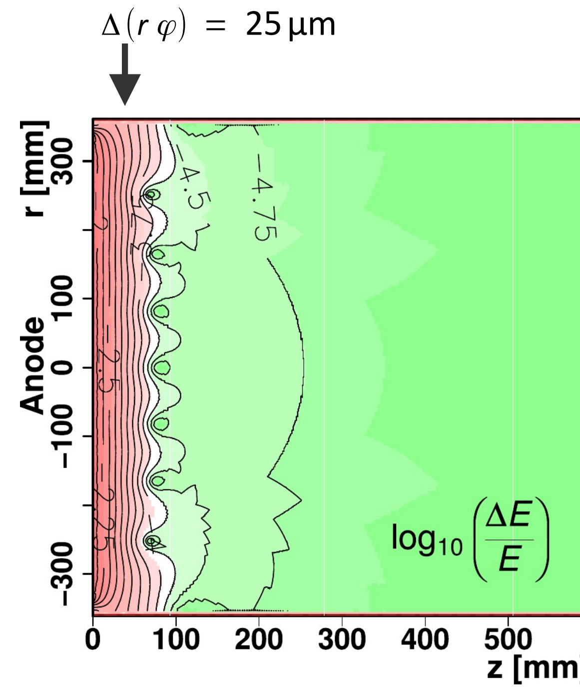


doi: 10.3204/DESY-THESIS-2010-015

# The Importance of Flat GEMs

- GEM deflections affect field homogeneity
- drift field distortions introduce E×B effects
  - can deteriorate spatial resolution
- inter-GEM fields influence GEM transparency for electrons
- non-uniformity introduces variations of effective gain

→ minimise deflection to not affect momentum & dE/dx measurement

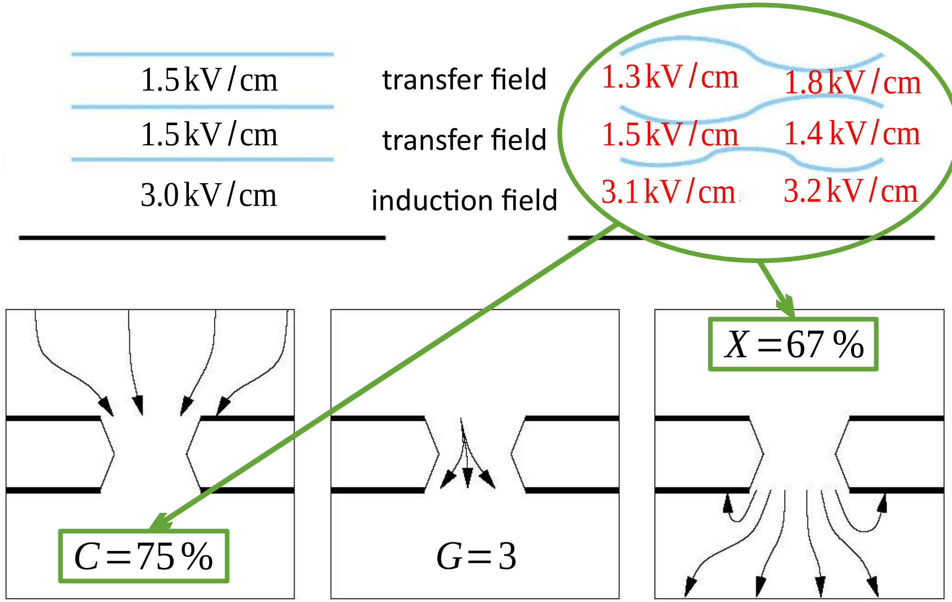


doi: 10.3204/DESY-THESIS-2010-015

# A new GEM Mounting Tool

- typically GEMs are mounted under strong tension → not possible due to thin frames
- mounting without pre-tension → deflections of GEM foils larger than tolerable
  - inherent to design or mounting process?
- developed & commissioned special mounting tool
- measure GEM flatness to compare old and new process

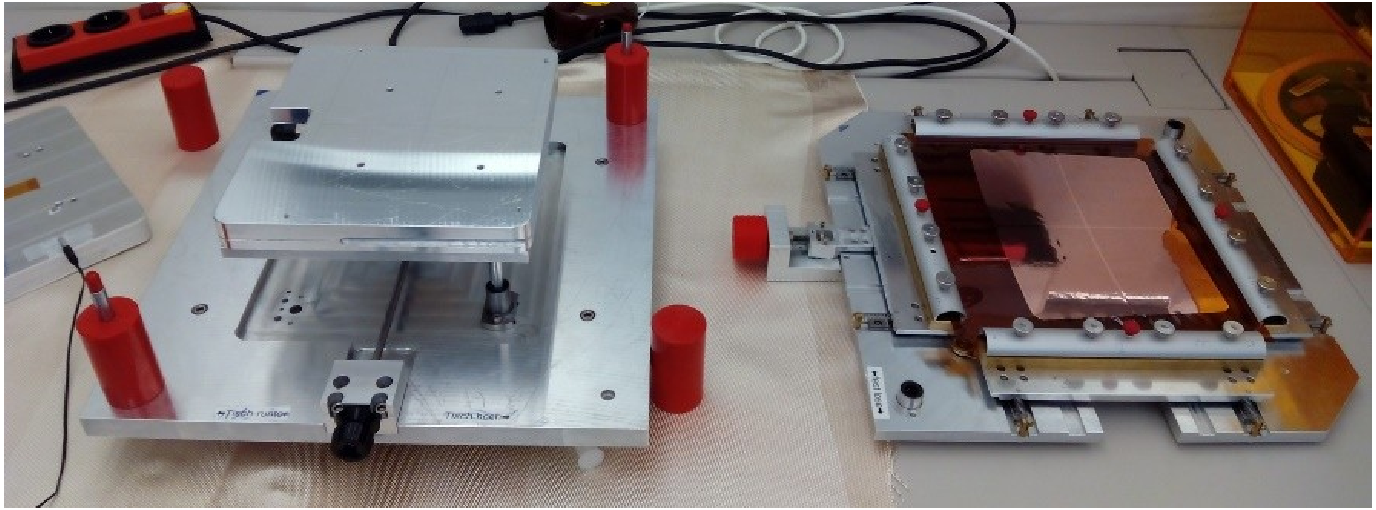

# Flatness Measurement Setup

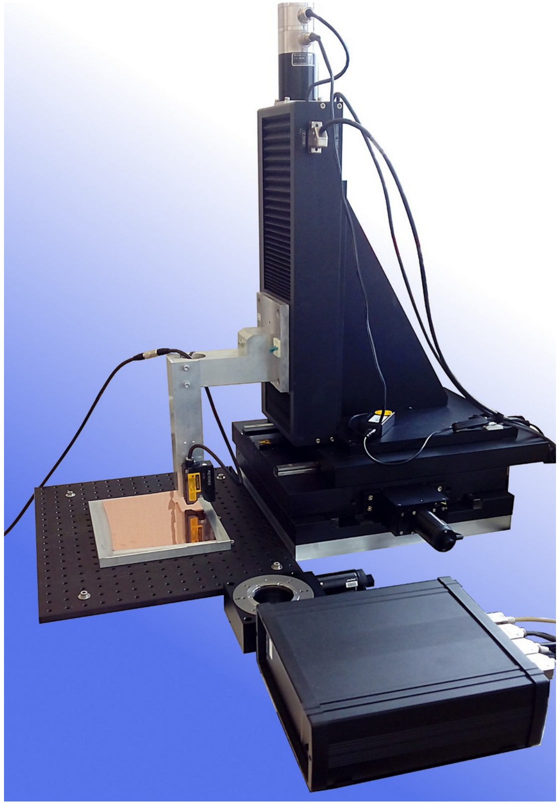

# Example Measurements

OLD PROCESS

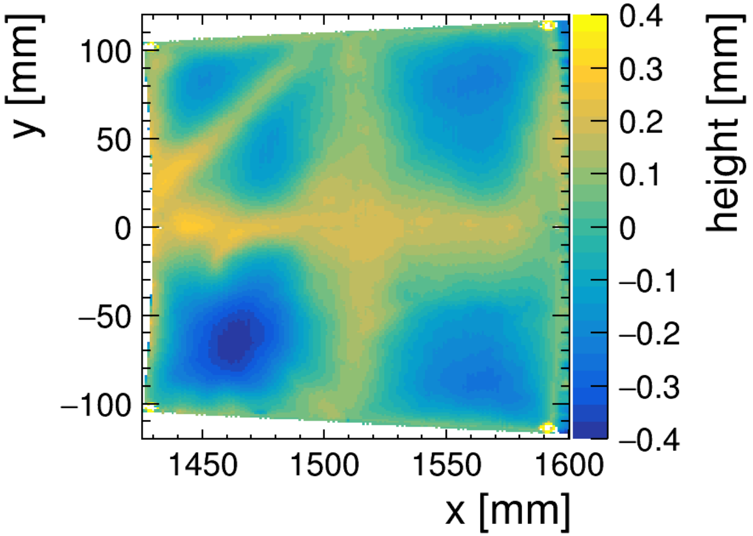


TOOL ASSISTED PROCESS

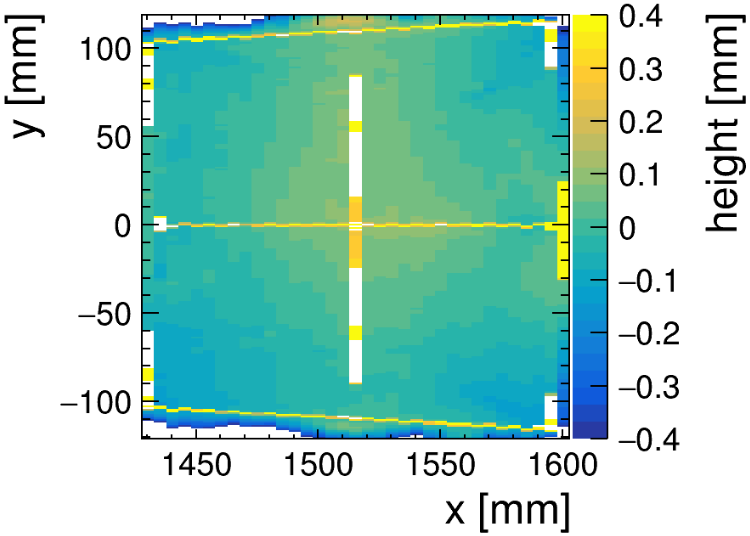

# GEM Flatness Comparison

- measurement setup:
  xyz-stage & laser displacement sensor
- sample size:
  - old process: 5 GEMs
  - tool assisted: 7 GEMs
- tool reduces deflections by factor 3
- location of largest deflections
  - manual: centre of frame cells
  - tool assisted: close to the frame
  - → flatness now limited by frames

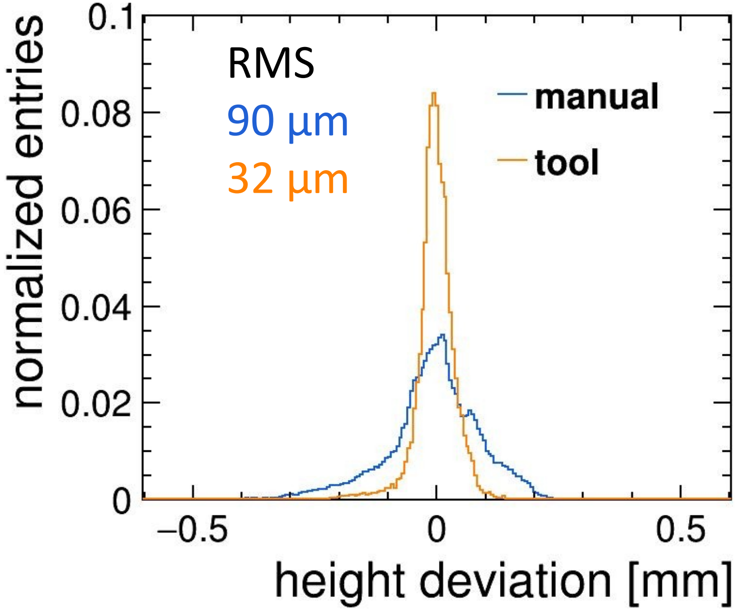

# Testbeam Measurement

- measurements to test new modules
  - extensive validation of previous results
    - spatial resolution
    - signal shape
    - environmental / systemic effects
  - new measurement: dE/dx resolution

- DESY II Test Beam: 5 GeV electrons
- 1 T solenoid magnet PCMag
- large TPC prototype (LPTPC)
- measurements cover full sensitive volume

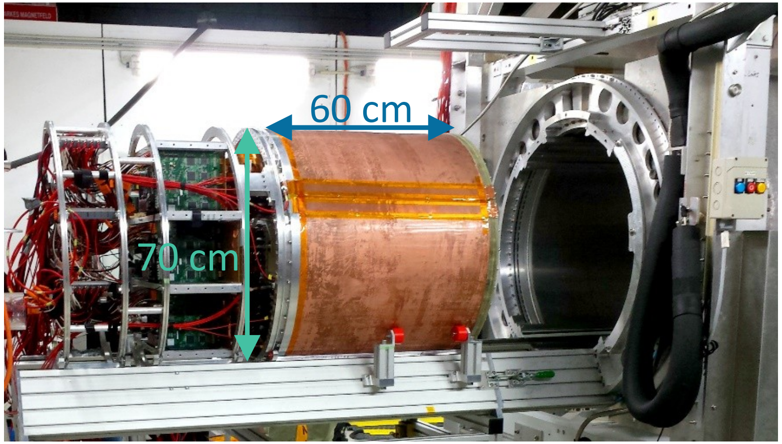

# Testbeam Measurement

- measurements to test new modules
  - extensive validation of previous results
    - spatial resolution
    - signal shape
    - environmental / systemic effects
  - new measurement: dE/dx resolution

- DESY II Test Beam: 5 GeV electrons
- 1 T solenoid magnet PCMag
- large TPC prototype (LPTPC)
- measurements cover full sensitive volume

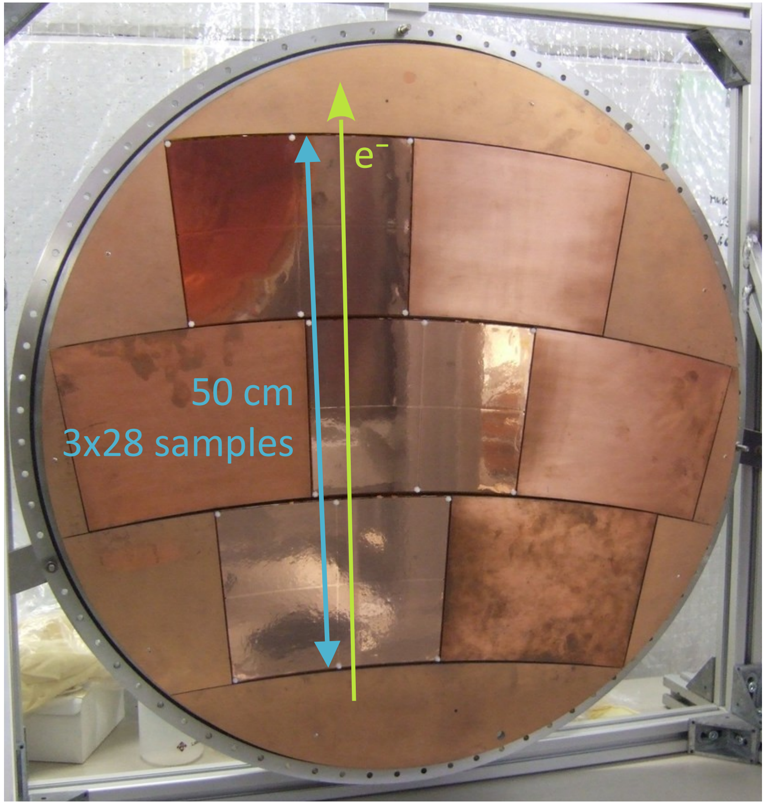

# Data Reconstruction

- readout based on ALTRO chip
  - 10 bit ADC
  - 20 MHz sampling rate
- pulse finding looks for charge peaks in each channel
  - configurable threshold parameters
- hit finding combines neighboring pulses based on charge
  - position calculated from charge-weighted mean
- track finding using Hough transformation
- track fitting using GBL

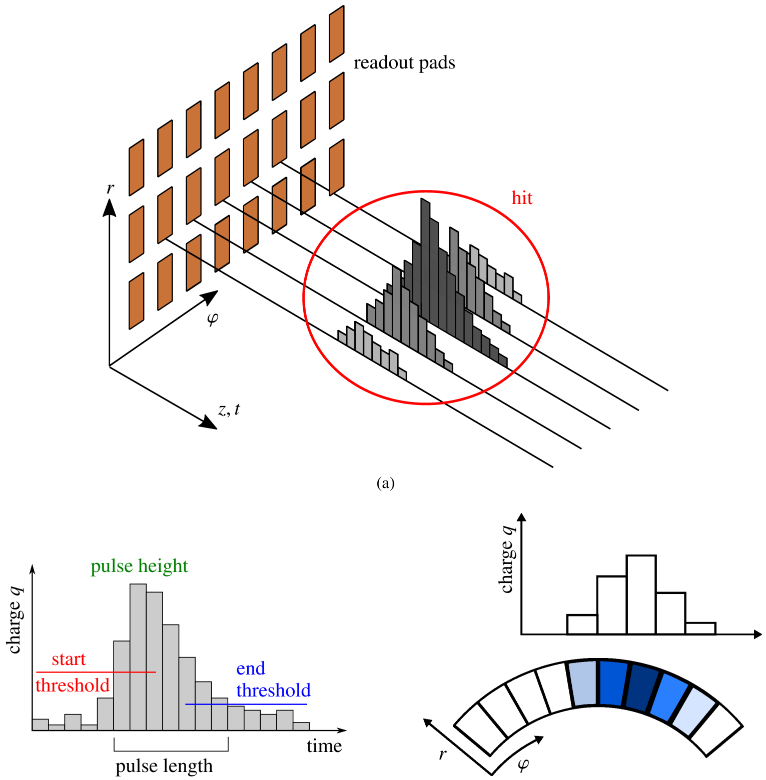

(a)
(b) pulse identification
(c) hit identification

doi: 10. 3204/PUBDB-2016-02659

# Signal Shape Measurements

- charge distribution on readout
  - gives information on shape of electron cloud
  - informs parameters for pulse & hit finding
- transverse: pad-response function (PRF)
  - convolution of pad pitch & charge cloud width
  - used to determine transverse diffusion
    - $\sigma_{PRF} = \sqrt{(\sigma_{PRF,0})^2 + (D_t)^2 \cdot z}$
- longitudinal: signal rise time
  - related to length of charge cloud
- both indicate smaller size for new modules
  → consistent with smaller distortions due to flatter GEMs
  - excluded other effects:
    - gas composition & contamination
    - environmental & system effects

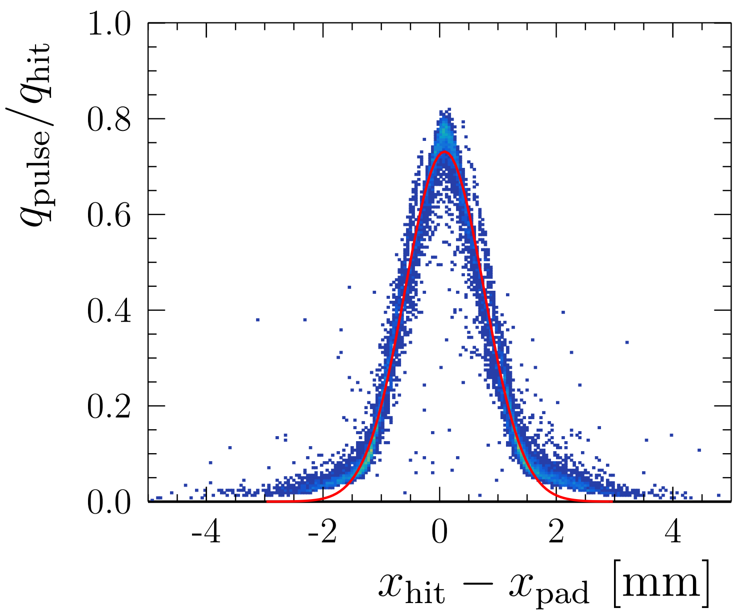

# Signal Shape Measurements

- charge distribution on readout
  - gives information on shape of electron cloud
  - informs parameters for pulse & hit finding
- transverse: pad-response function (PRF)
  - convolution of pad pitch & charge cloud width
  - used to determine transverse diffusion
    - $\sigma_{PRF} = \sqrt{(\sigma_{PRF,0})^2 + (D_t)^2 \cdot z}$
- longitudinal: signal rise time
  - related to length of charge cloud
- both indicate smaller size for new modules
  → consistent with smaller distortions due to flatter GEMs
  - excluded other effects:
    - gas composition & contamination
    - environmental & system effects

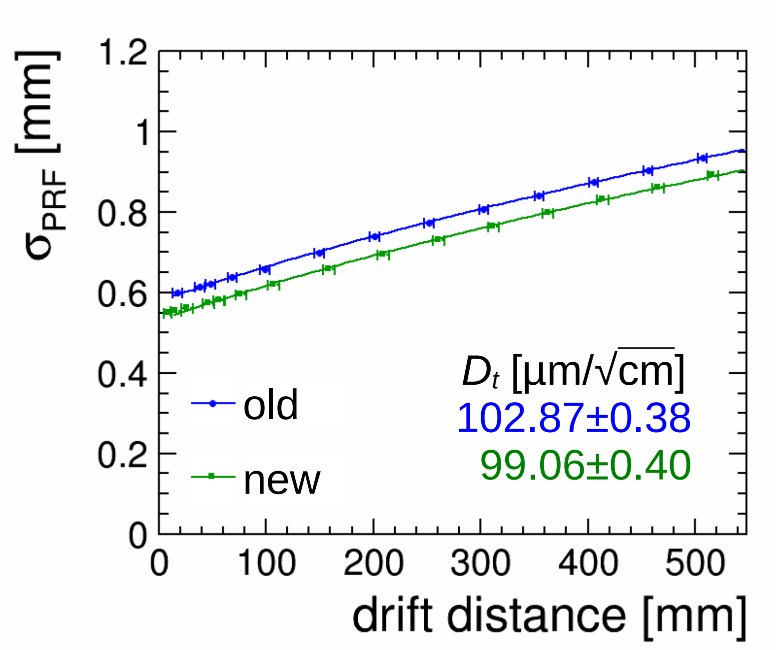

# Signal Shape Measurements

- charge distribution on readout
  - gives information on shape of electron cloud
  - informs parameters for pulse & hit finding
- transverse: pad-response function (PRF)
  - convolution of pad pitch & charge cloud width
  - used to determine transverse diffusion
    - $\sigma_{PRF} = \sqrt{(\sigma_{PRF,0})^2 + (D_t)^2 \cdot z}$
- longitudinal: signal rise time
  - related to length of charge cloud
- both indicate smaller size for new modules
  → consistent with smaller distortions due to flatter GEMs
  - excluded other effects:
    - gas composition & contamination
    - environmental & system effects

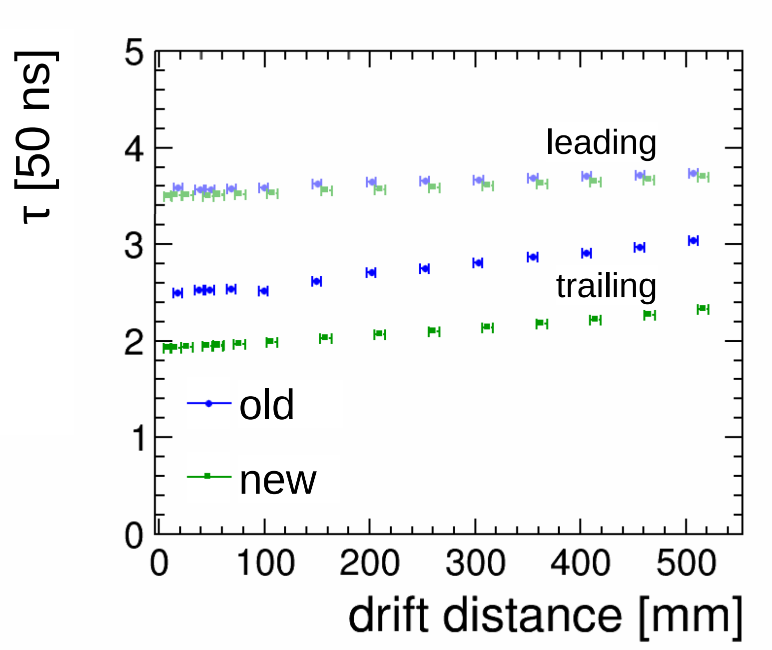

# Spatial Resolution Measurement

- spatial resolution determined from distribution of track residuals
- depends on drift distance $z$
  - $\sigma_{r\varphi} = \sqrt{(\sigma_{r\varphi,0})^2 + \frac{(D_t)^2}{N_{\text{eff}} \cdot e^{-Az}} \cdot z}$
  - deteriorates due to diffusion
  - electron attachment to oxygen contamination
- diffusion coefficient from PRF measurement used as input for fit
- fit result can be used to extrapolate to ILD
  - higher magnetic field → lower diffusion
  - no significant attachment expected
- 100 µm resolution at full drift can be reached

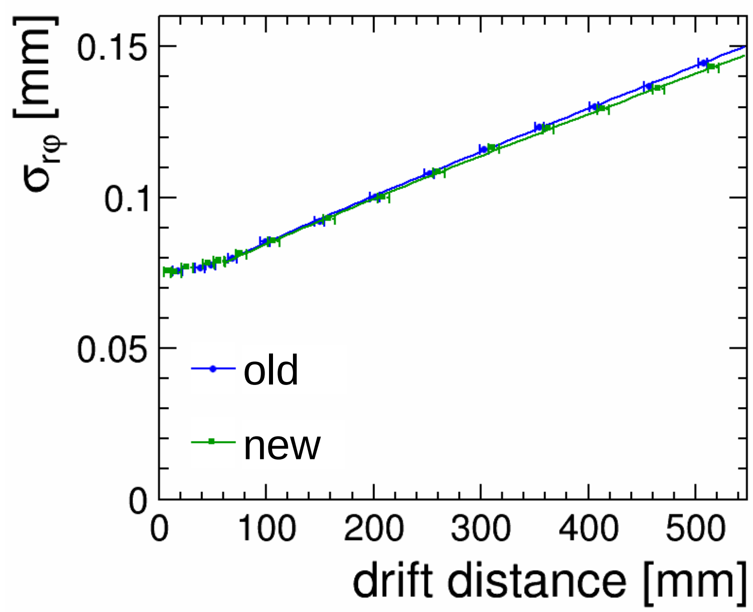

# Spatial Resolution Measurement

- spatial resolution determined from distribution of track residuals
- depends on drift distance *z*
  - $\sigma_{r\varphi} = \sqrt{(\sigma_{r\varphi,0})^2 + \frac{(D_t)^2}{N_{\text{eff}} \cdot e^{-Az}} \cdot z}$
  - deteriorates due to diffusion
  - electron attachment to oxygen contamination
- diffusion coefficient from PRF measurement used as input for fit
- fit result can be used to extrapolate to ILD
  - higher magnetic field → lower diffusion
  - no significant attachment expected
- 100 µm resolution at full drift can be reached

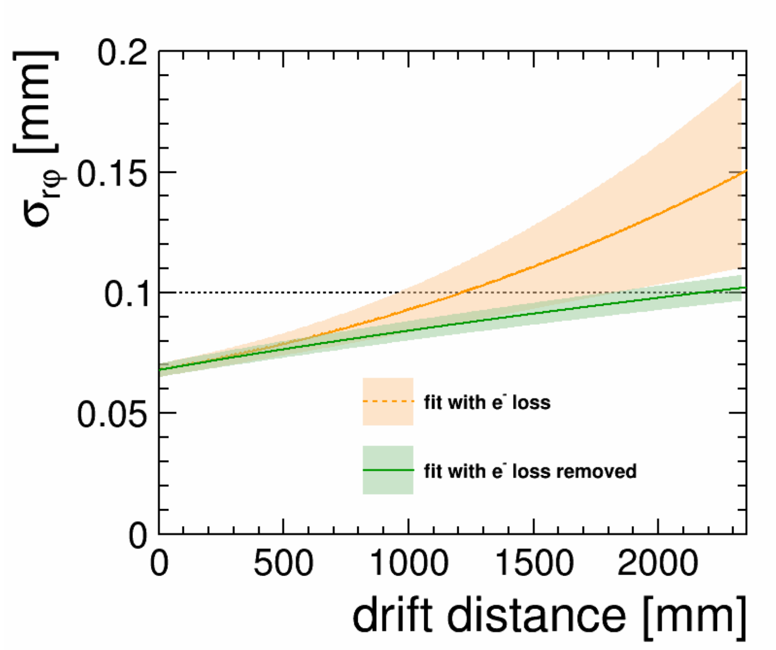

# Determining the d$E$/d$x$ Resolution

- measure $Q/\Delta x$ for each hit
  - energy loss $\Delta E \propto Q$
- apply charge calibration
- Landau tail affects average $Q$

- best estimator:
  → 75 % truncated mean
- resolution from RMS of distribution

- resolution is constant
  → average over several runs
- relative resolution: ~9%
  - for 56 valid hits per track

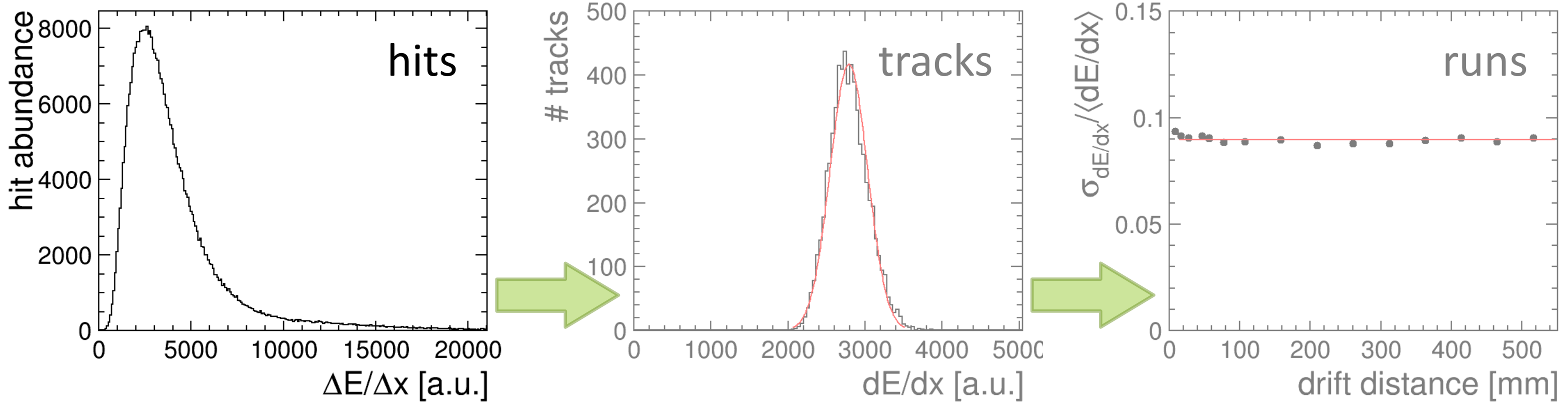

# Determining the d$E$/d$x$ Resolution

- measure $Q/\Delta x$ for each hit
  - energy loss $\Delta E \propto Q$
- apply charge calibration
- Landau tail affects average $Q$

- best estimator:
  → 75 % truncated mean
- resolution from RMS of distribution

- resolution is constant
  → average over several runs
- relative resolution: ~9%
  - for 56 valid hits per track

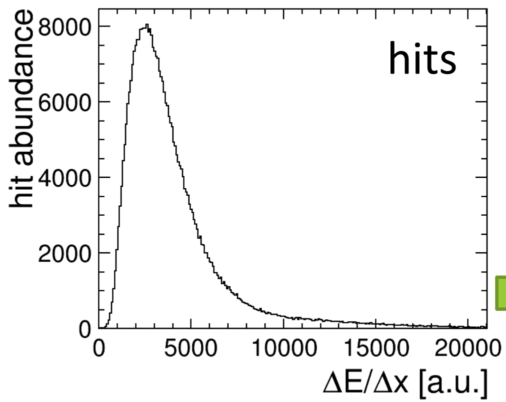


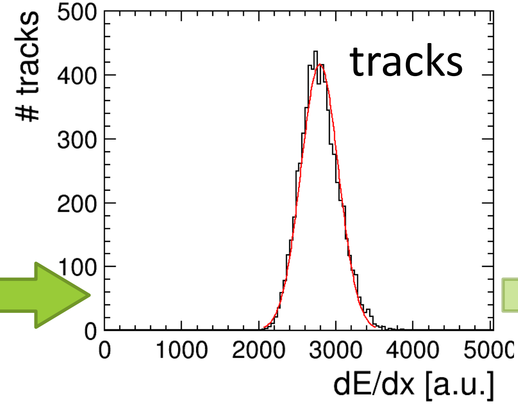


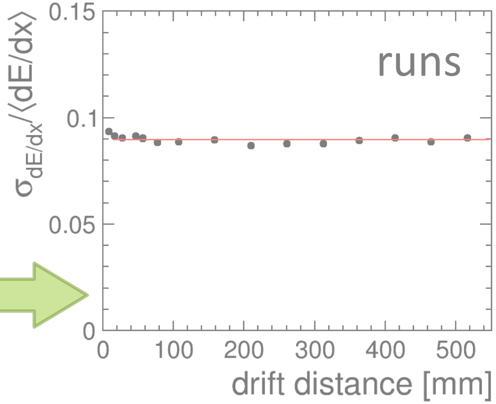

# Determining the d$E$/d$x$ Resolution

- measure $Q/\Delta x$ for each hit
  - energy loss $\Delta E \propto Q$
- apply charge calibration
- Landau tail affects average $Q$

- best estimator:
  → 75 % truncated mean
- resolution from RMS of distribution

- resolution is constant
  → average over several runs
- relative resolution: ~9%
  - for 56 valid hits per track

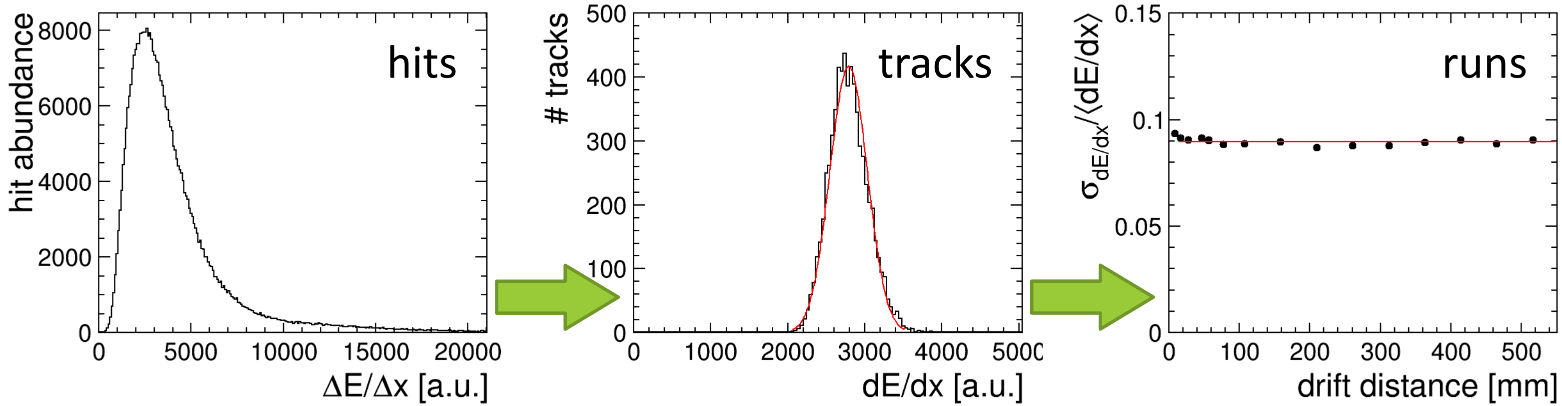

# Extrapolation to ILD

- extrapolate from LPTPC to ILD TPC
  - 56 hits to 220 hits
- dE/dx resolution scales with number of hits
  - power law $\sigma_0 \cdot N^{-k}, k < 0.5$
- idea: combine hits from multiple tracks
  → pseudo tracks of arbitrary length
- power law fit finds $k$ = 0.48
- resolution at 220 hits: 4.8%
- fulfills ILD goal of 5 %

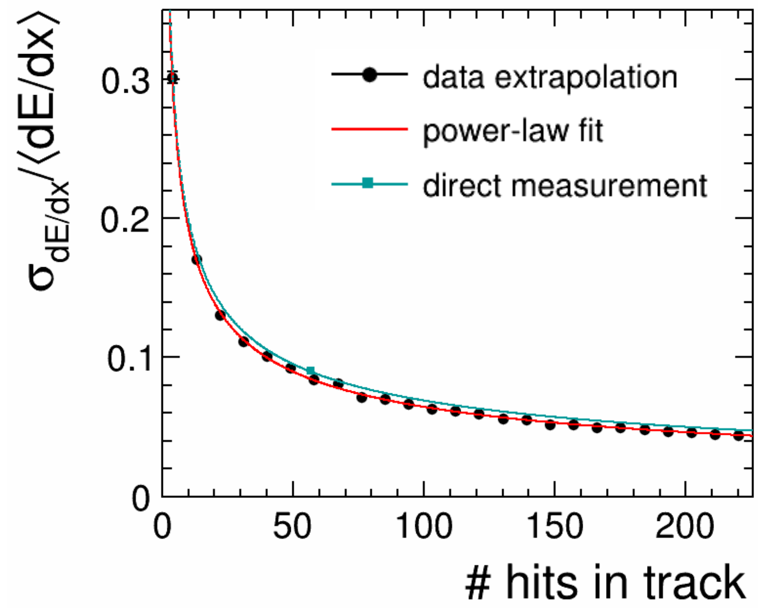

# Summary

- the ILC is a mature project with an extensive physics case
- the ILD concept is able to provide the required measurement precision
  - supported by detailed simulations & prototype tests
- the GEM + pad based TPC readout fulfills the requirements of the ILD TPC

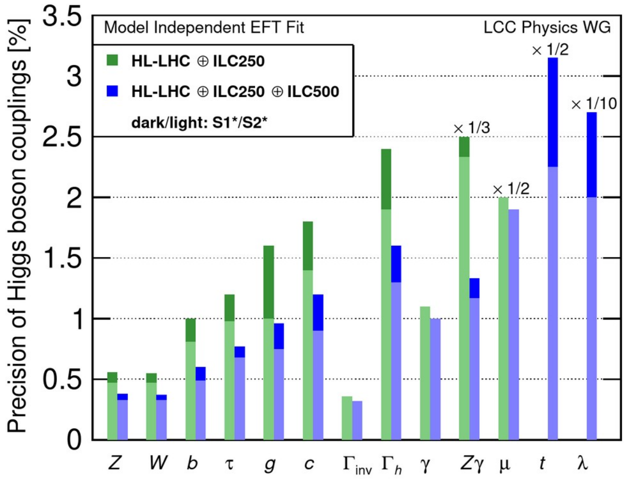


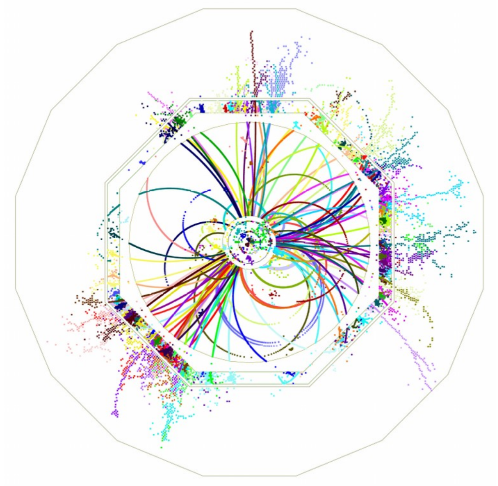

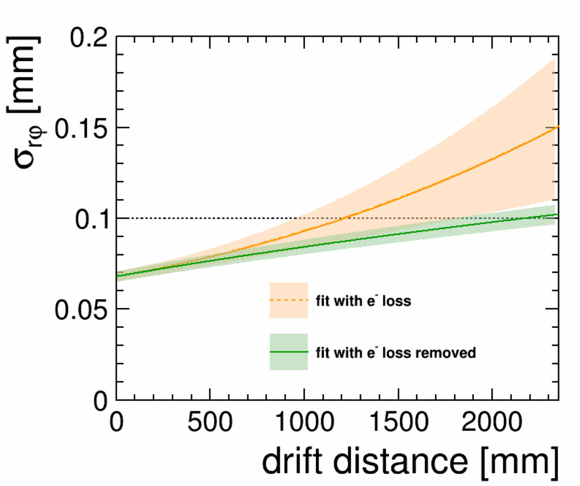

# Backup

# Why $e^+e^-$?

- cleanliness:
  - no pileup
  - no underlying event

→ more benign radiation environment
  - allows to optimise detector performance

- cross-section "democracy"
  - Higgs cross-section ~1% of total
  - typical BSM cross-sections: ~0.1% - 1% of total

→ no trigger necessary
  - all events can be analysed
  - rare processes & unusual signatures detectable

- know / fully reconstructible initial / final state
  - well defined centre-of-mass energy

→ reduces required model assumptions
→ allows study of spin dependence

- no QCD corrections to cross-section calculations

→ much more precise theory predictions
  - indirect searches for new physics to O(10 TeV)

# ILC Specifications

| Quantity | Symbol | Unit | Initial | $\mathcal{L}$ Upgrade | Z pole | Upgrades | | |
|---|---|---|---|---|---|---|---|---|
| Centre of mass energy | $\sqrt{s}$ | GeV | 250 | 250 | 91.2 | 500 | 250 | 1000 |
| Luminosity | $\mathcal{L}$ | $10^{34}\text{cm}^{-2}\text{s}^{-1}$ | 1.35 | 2.7 | 0.21/0.41 | 1.8/3.6 | 5.4 | 5.1 |
| Polarization for $e^-/e^+$ | $P_-(P_+)$ | % | 80(30) | 80(30) | 80(30) | 80(30) | 80(30) | 80(20) |
| Repetition frequency | $f_\text{rep}$ | Hz | 5 | 5 | 3.7 | 5 | 10 | 4 |
| Bunches per pulse | $n_\text{bunch}$ | 1 | 1312 | 2625 | 1312/2625 | 1312/2625 | 2625 | 2450 |
| Bunch population | $N_\text{e}$ | $10^{10}$ | 2 | 2 | 2 | 2 | 2 | 1.74 |
| Linac bunch interval | $\Delta t_\text{b}$ | ns | 554 | 366 | 554/366 | 554/366 | 366 | 366 |
| Beam current in pulse | $I_\text{pulse}$ | mA | 5.8 | 8.8 | 5.8/8.8 | 5.8/8.8 | 8.8 | 7.6 |
| Beam pulse duration | $t_\text{pulse}$ | $\mu$s | 727 | 961 | 727/961 | 727/961 | 961 | 897 |
| Average beam power | $P_\text{ave}$ | MW | 5.3 | 10.5 | $1.42/2.84^{*)}$ | 10.5/21 | 21 | 27.2 |
| RMS bunch length | $\sigma^*_\text{z}$ | mm | 0.3 | 0.3 | 0.41 | 0.3 | 0.3 | 0.225 |
| Norm. hor. emitt. at IP | $\gamma\epsilon_\text{x}$ | $\mu$m | 5 | 5 | 6.2 | 5 | 5 | 5 |
| Norm. vert. emitt. at IP | $\gamma\epsilon_\text{y}$ | nm | 35 | 35 | 48.5 | 35 | 35 | 30 |
| RMS hor. beam size at IP | $\sigma^*_\text{x}$ | nm | 516 | 516 | 1120 | 474 | 516 | 335 |
| RMS vert. beam size at IP | $\sigma^*_\text{y}$ | nm | 7.7 | 7.7 | 14.6 | 5.9 | 7.7 | 2.7 |
| Luminosity in top 1 % | $\mathcal{L}_{0.01}/\mathcal{L}$ | | 73 % | 73 % | 99 % | 58.3 % | 73 % | 44.5 % |
| Beamstrahlung energy loss | $\delta_\text{BS}$ | | 2.6 % | 2.6 % | 0.16 % | 4.5 % | 2.6 % | 10.5 % |
| Site AC power | $P_\text{site}$ | MW | 111 | 128 | 94/115 | 173/215 | 198 | 300 |
| Site length | $L_\text{site}$ | km | 20.5 | 20.5 | 20.5 | 31 | 31 | 40 |

# dE/dx Comparison: ALICE & ILD

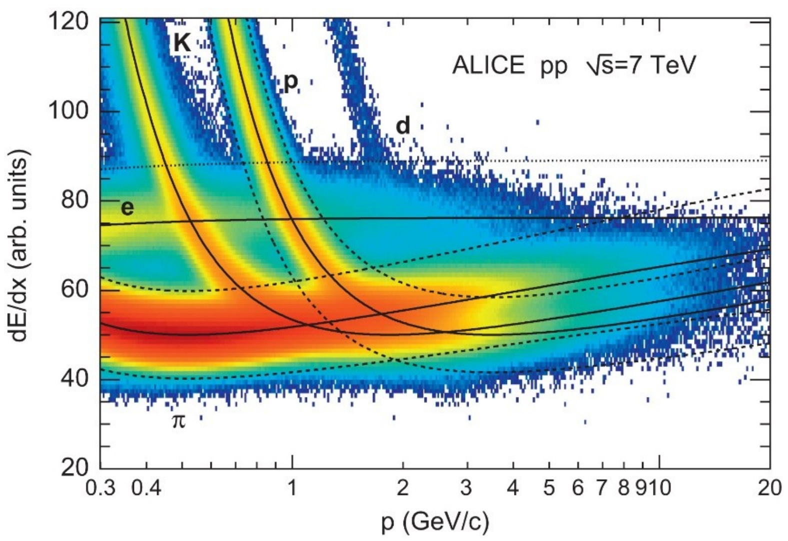


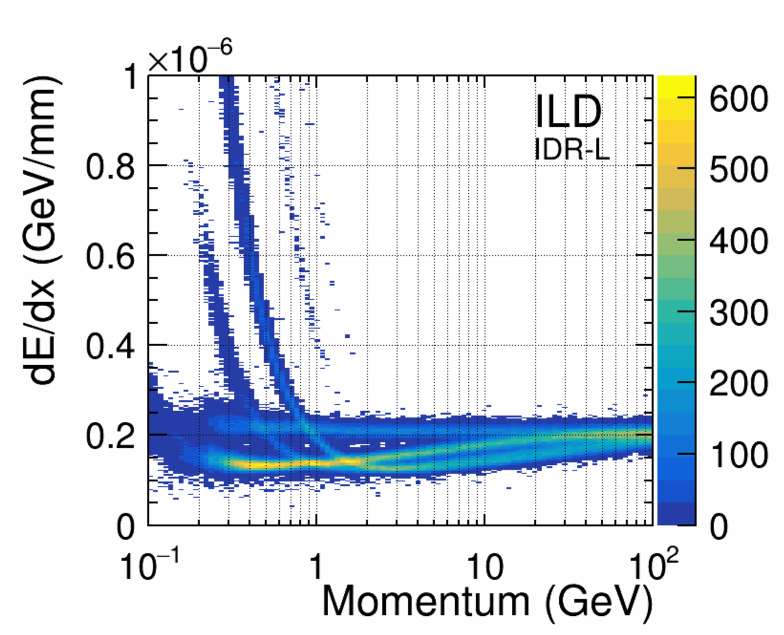

# ILD Tracking Efficiency

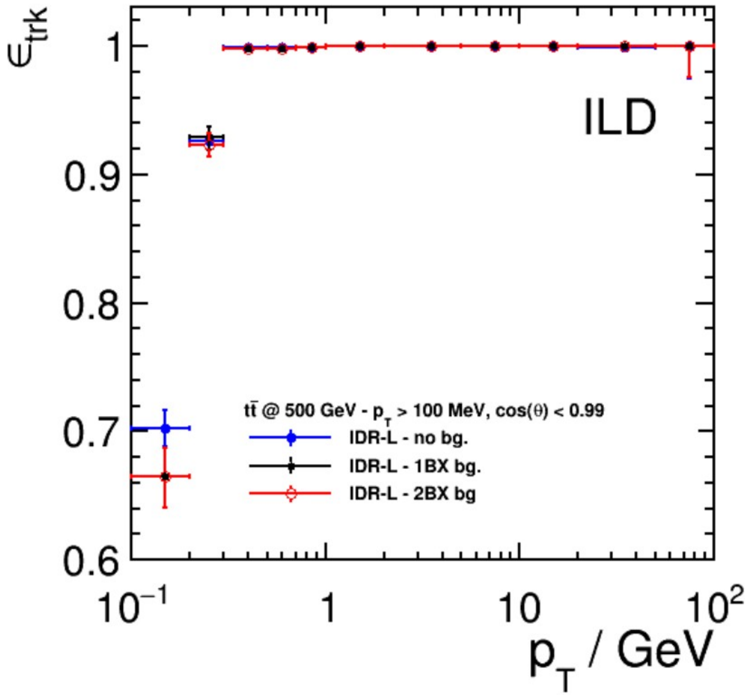


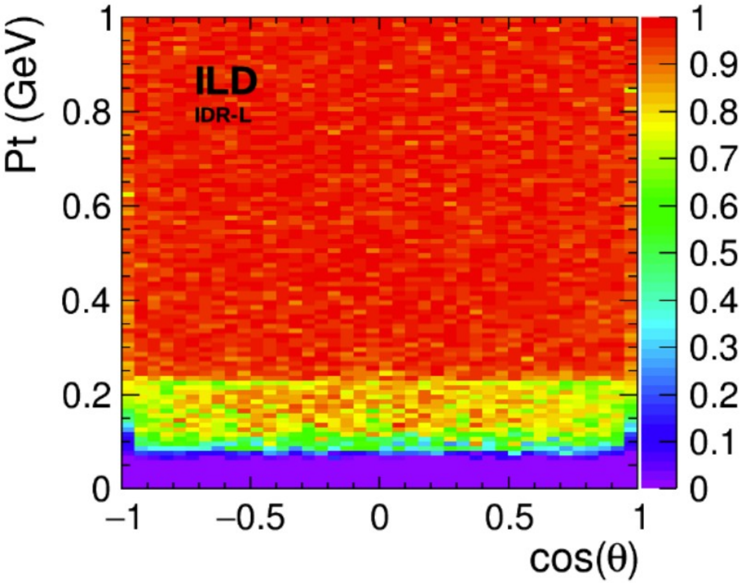

# ALICE TPC – Gain Map

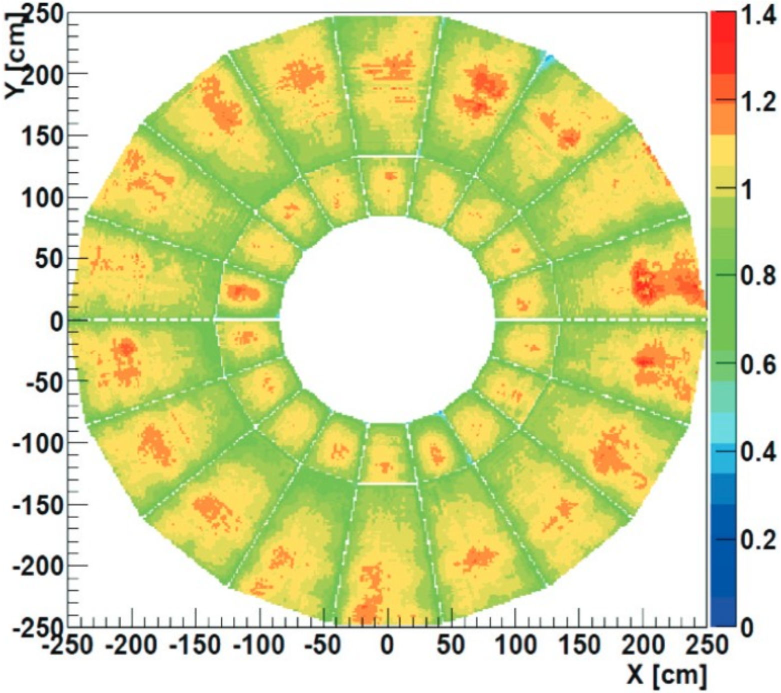


- MWPC readout

# Gaseous Detector Comparison

| experiment | chamber type | depth [cm x bar] | samples | dE/dx resolution [%] | |
|---|---|---|---|---|---|
| ILD | TPC | 135 | 220 | 4.7 (iso., Fermi) | |
| DELPHI | TPC | 80 | 192 | 5.7 (Fermi plateau) | 6.2 (MIP) |
| ALEPH | TPC | 150 | 21 | 4.6 (Fermi plateau) | |
| OPAL | drift chamber | 160 x 3.5 | 159 | 3.1 (iso., Fermi) | 3.8 (MIP, jet) |
| STAR | TPC | 150 | 45 | 6.7 | |
| ALICE | TPC | 160 | 159 | 5.5 (isolated) | 8-12 (high density) |

# PID Technologies

- basic grouping with PF: charged hadrons, neutral hadrons, photons, electrons, muons
- gaseous detectors (TPC, wire/drift chambers): dE/dx
  - much worse in silicon detectors: only few samples
- Time of Flight (TOF)
  - only for low momenta (< 10 GeV)
- Cherenkov detectors: RICH, DIRC, TOP
- transition radiation detectors (TRD)

(bracketed: gaseous detectors through TRD) only charged particles

# Time of Flight PID

- ECAL single-hit time resolution: 50 ps
- average over 10 first ECAL hits

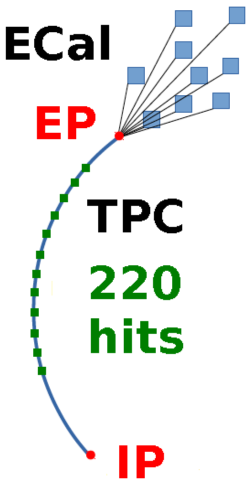


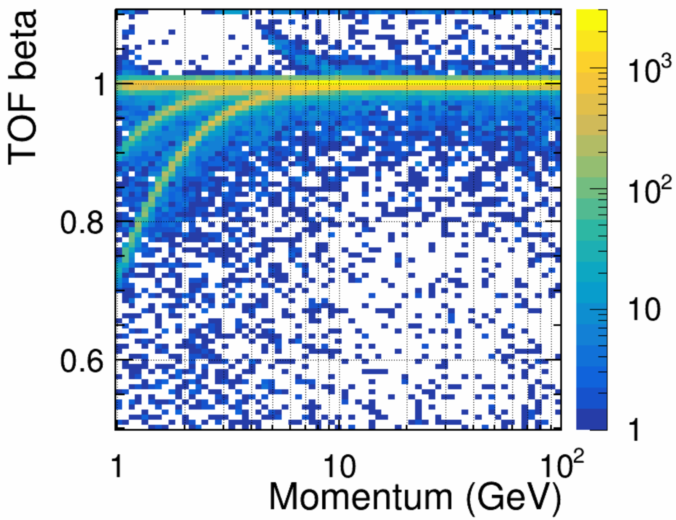


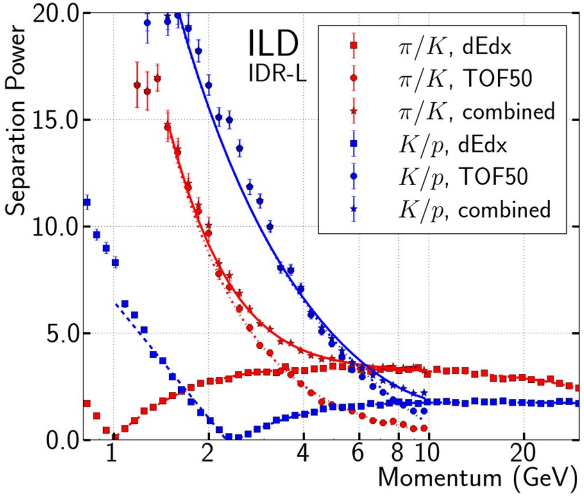


[U. Einhaus, 2021]

# Average Deflection Comparison

MANUAL PROCESS

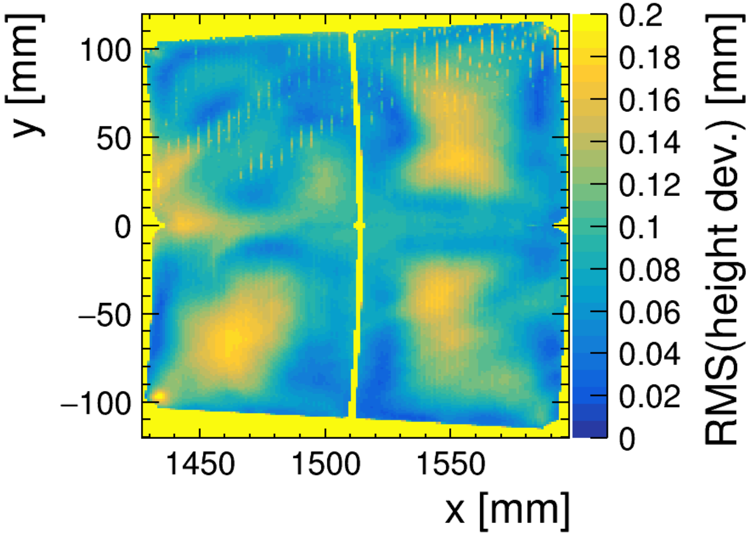


TOOL ASSISTED PROCESS

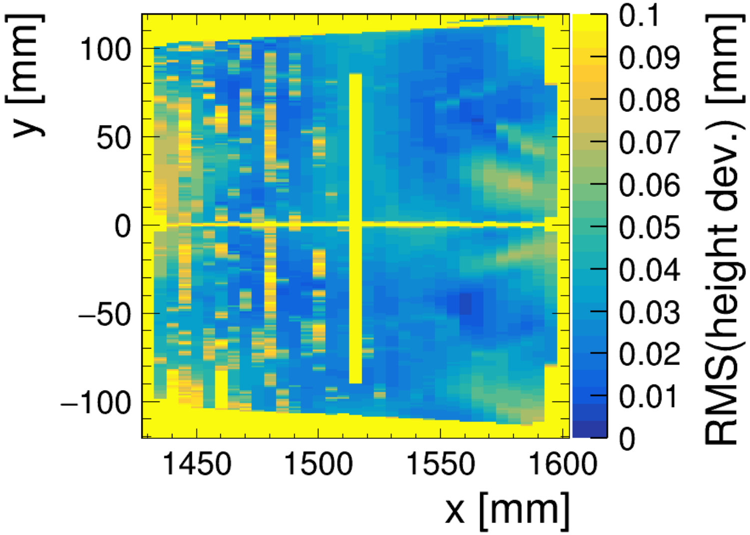

# Gain Calculation

- calculation of triple GEM stack gain
  - based on parametrised measurements
  - depends on gas mixture and E/B fields
  - T2K gas: 95% Ar : 3% $CF_4$ : 2% $HC(CH_3)_3$
    - also used in test beam
- build stacks of 3 GEMs from measured deflection profiles
  - increase statistics by mirroring and inverting
  - different stacks: 2880 (manual), 8736 (tool)
- deflections modulate electric fields locally
- GEM mounting tool reduces gain fluctuations by factor 2.7

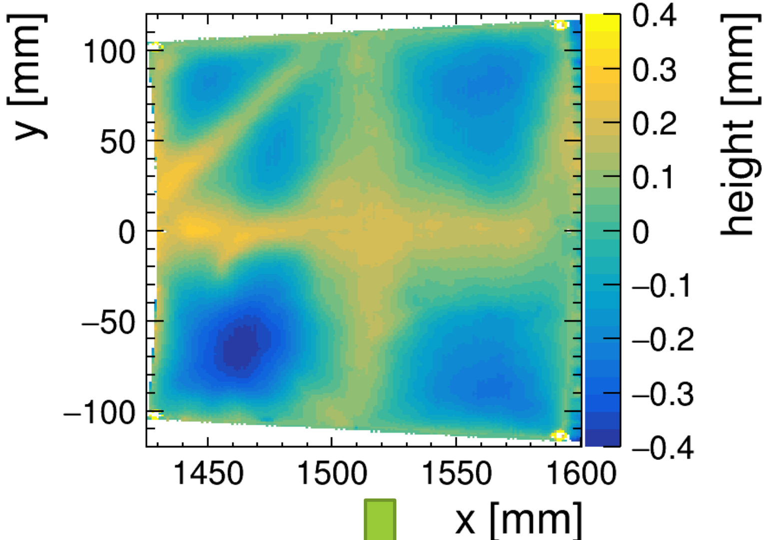


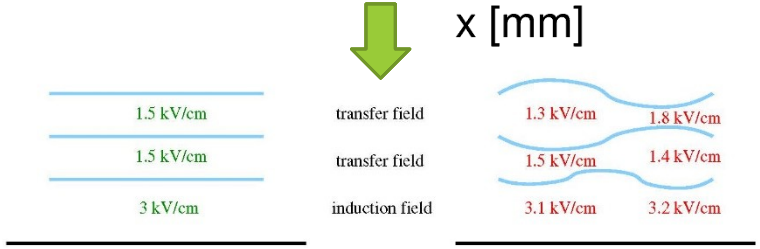

# Gain Calculation

- calculation of triple GEM stack gain
  - based on parametrised measurements
  - depends on gas mixture and E/B fields
  - T2K gas: 95% Ar : 3% $CF_4$ : 2% $HC(CH_3)_3$
    - also used in test beam
- build stacks of 3 GEMs from measured deflection profiles
  - increase statistics by mirroring and inverting
  - different stacks: 2880 (manual), 8736 (tool)
- deflections modulate electric fields locally
- GEM mounting tool reduces gain fluctuations by factor 2.7

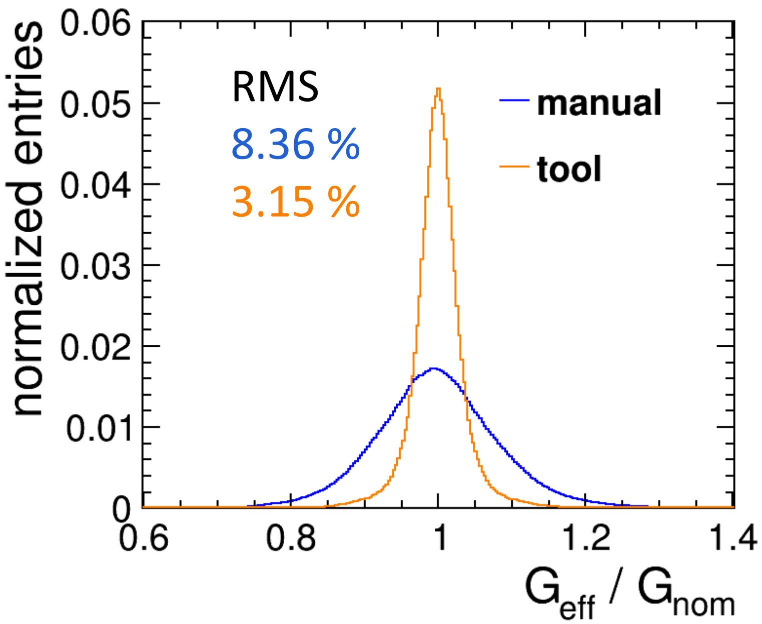

# Average Gain Deviation

MANUAL PROCESS

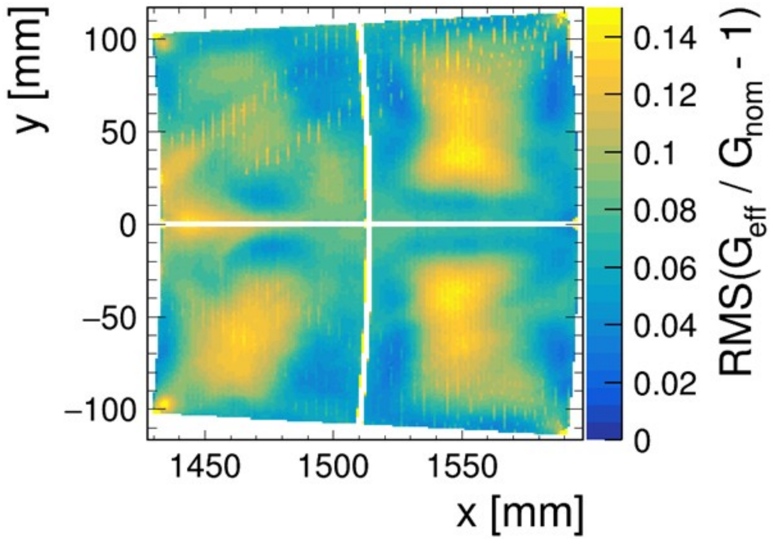


TOOL ASSISTED PROCESS

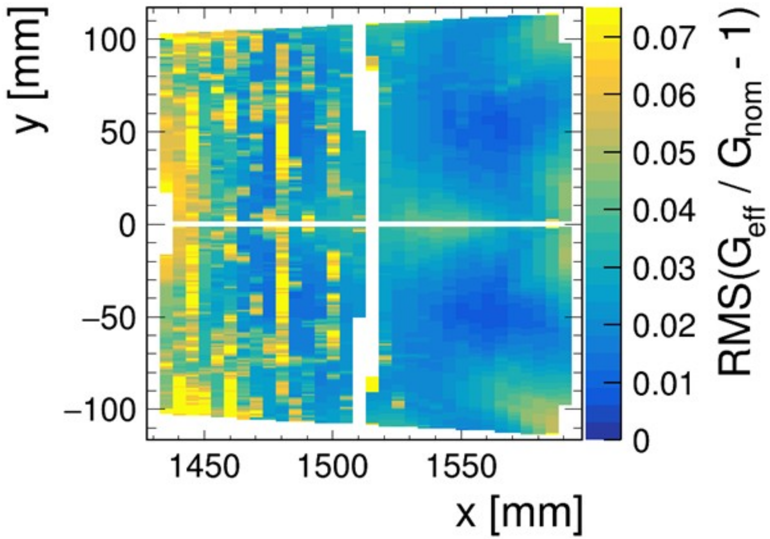

# Average Gain on Tracks

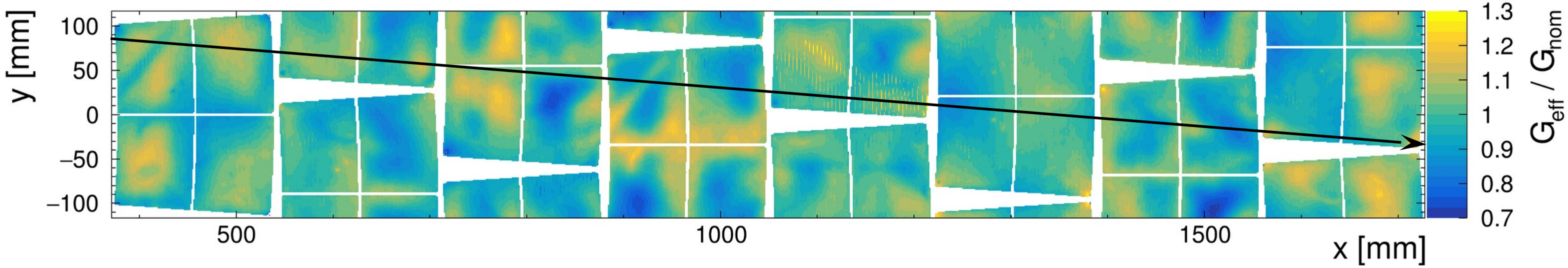


- build “ILD TPC sectors” from calculated gain maps
  - 8 modules each
- straight tracks from bins in first column to last
- calculate average gain for each track
- for ILD: fluctuations of 0.5 % tolerable after calibration
- 0.66 % is close → less demanding calibration

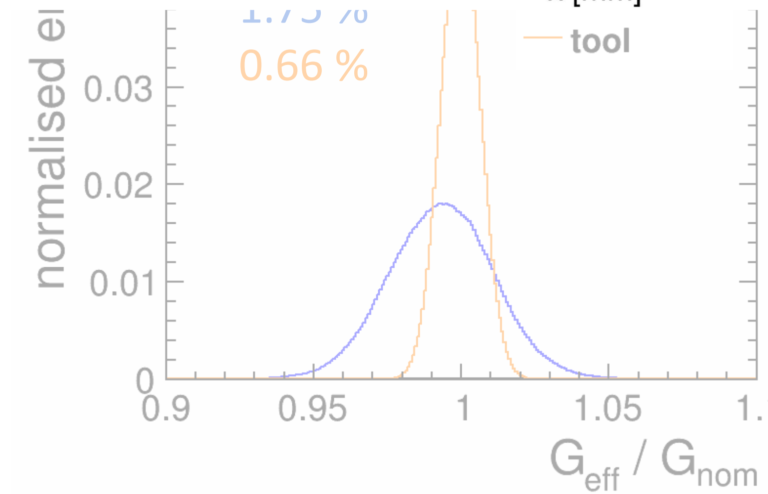

# Average Gain on Tracks

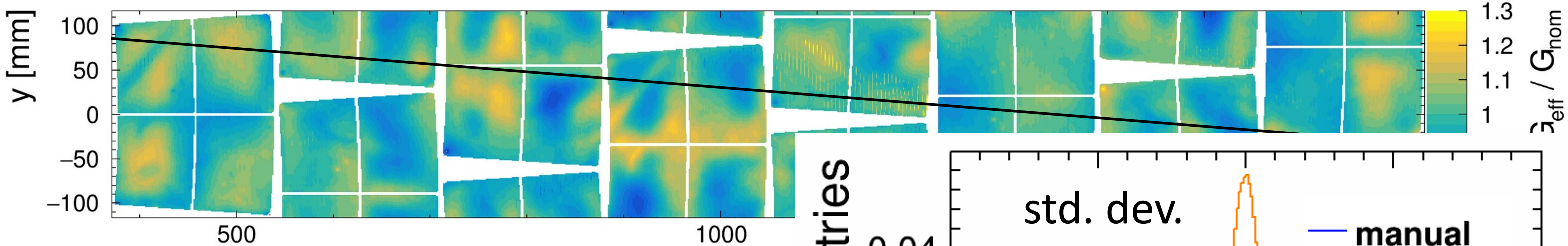


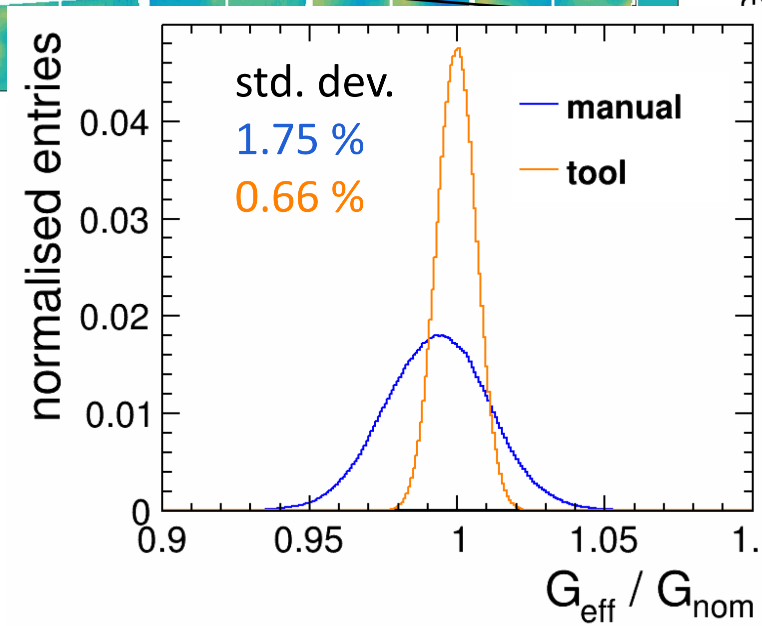


- build “ILD TPC sectors” from calculated gain maps
  - 8 modules each
- straight tracks from bins in first column to last
- calculate average gain for each track
- for ILD: fluctuations of 0.5 % tolerable after calibration
- 0.66 % is close → less demanding calibration

# Hit Selection for dE/dx

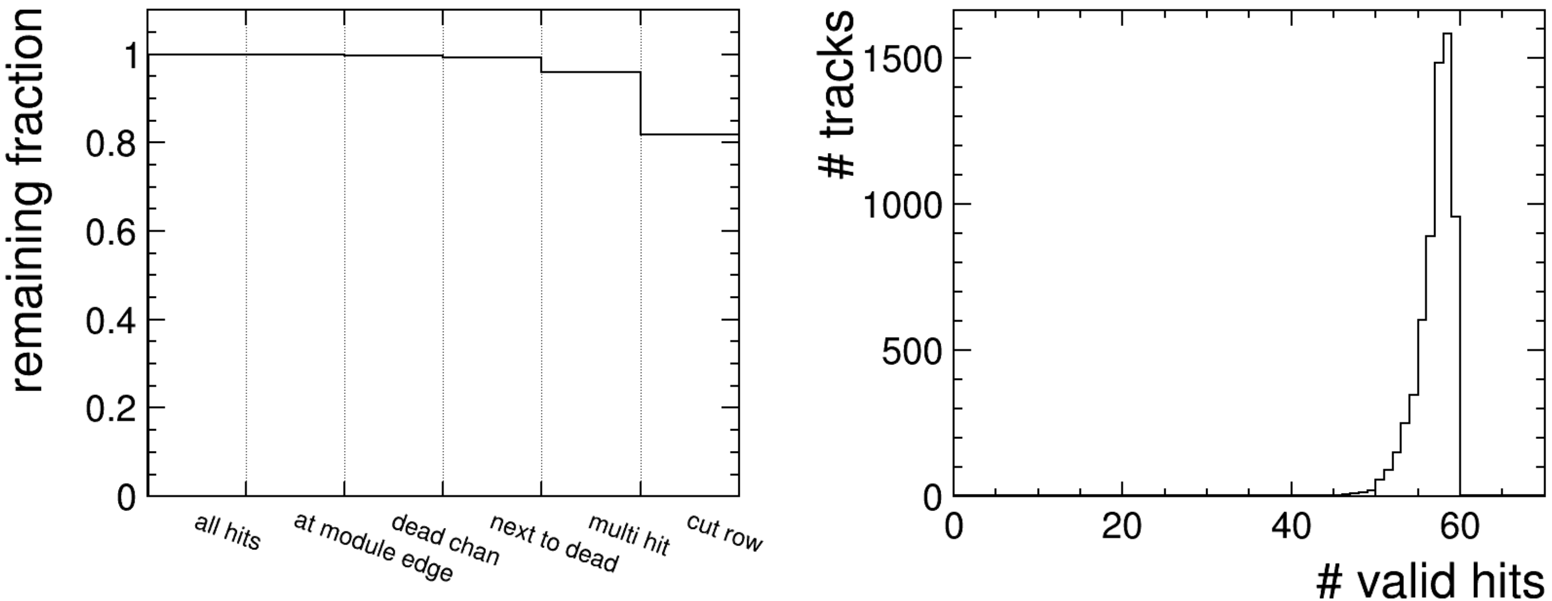


**(a)** Cumulative cut efficiency. **(b)** Number of valid hits.

**Figure 9.3.:** The effect of the hit quality cuts. (a) The efficiency of the cuts if applied successively. (b) The distribution of the resulting number of valid hits on a track after all cuts.

# Finding the Optimal Estimator

- suppress Landau tail of
- traditionally: truncated mean
  → optimise fraction
- transformed distribution
  - more compact and symmetric
- alternative: fit distribution including tail
  - reasonable descriptions: Landau and log-normal
- best resolution: truncated mean at 75 %
- fitting takes 10× more computing time

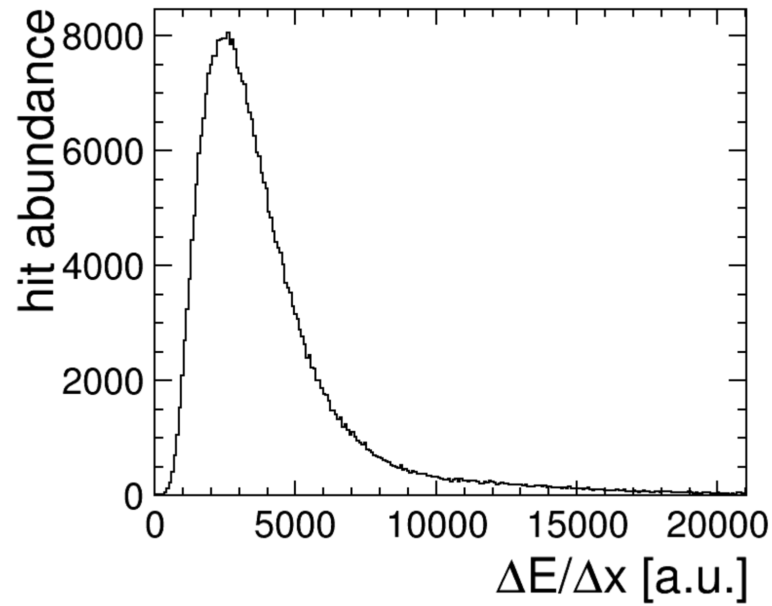

# Finding the Optimal Estimator

- suppress Landau tail of
- traditionally: truncated mean
  → optimise fraction
- transformed distribution
  - more compact and symmetric
- alternative: fit distribution including tail
  - reasonable descriptions: Landau and log-normal
- best resolution: truncated mean at 75 %
- fitting takes 10× more computing time

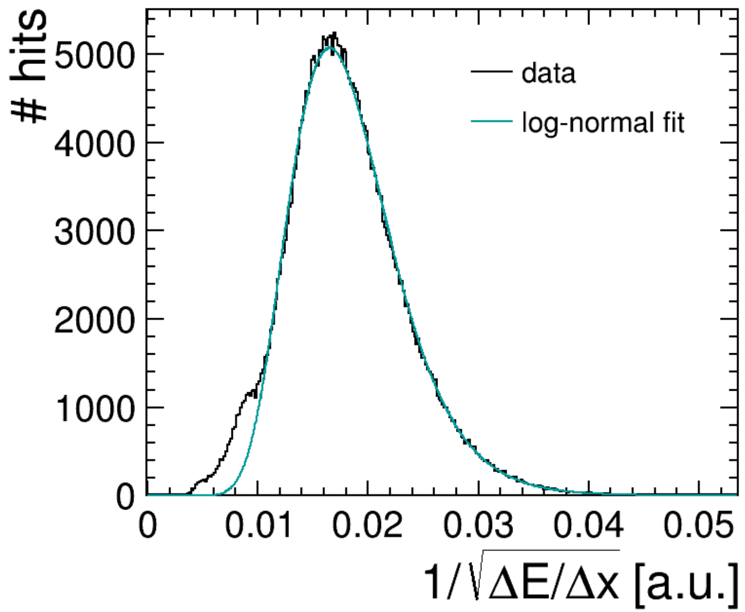

# Finding the Optimal Estimator

- suppress Landau tail of
- traditionally: truncated mean
  → optimise fraction
- transformed distribution
  - more compact and symmetric
- alternative: fit distribution including tail
  - reasonable descriptions: Landau and log-normal
- best resolution: truncated mean at 75 %
- fitting takes 10× more computing time

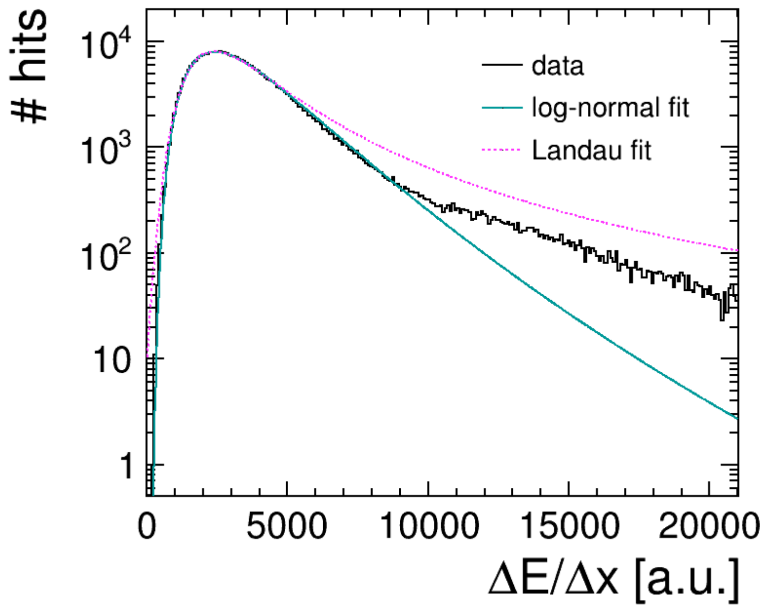

# Finding the Optimal Estimator

- suppress Landau tail of
- traditionally: truncated mean
  → optimise fraction
- transformed distribution
  - more compact and symmetric
- alternative: fit distribution including tail
  - reasonable descriptions: Landau and log-normal
- best resolution: truncated mean at 75 %
- fitting takes 10× more computing time

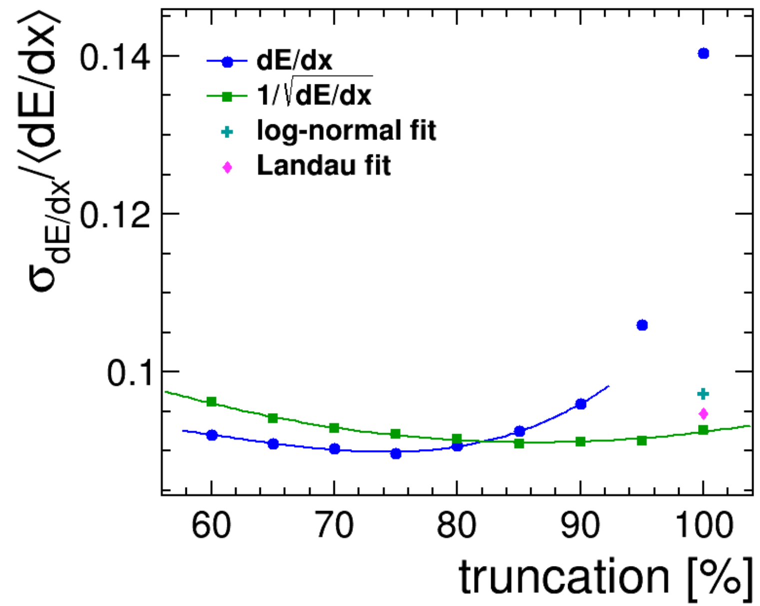

# Calibrating the Charge Measurement

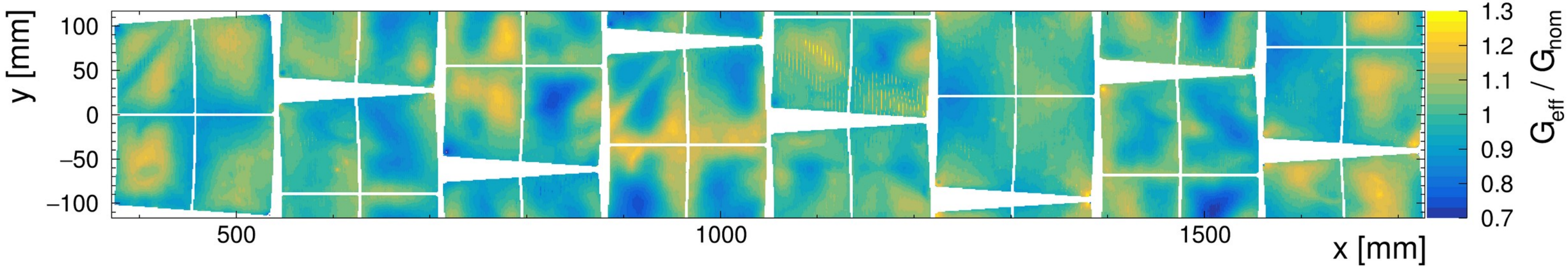


- correct local variations of charge measurement
  - due to electronics gain or gas gain
- in final experiment: dedicated calibration systems
  - electronics: calibration DAC
  - gas gain: radiation sources (,)
- not available in prototype setup
  → investigate alternatives
- electronics channel calibration:
  - induce charge by pulsing closest GEM
- gas gain correction:
  - use test beam data

# Electronics Channel Calibration

- idea: pulse GEM closest to pad board to induce charge
- pulses at various voltages
  → calibration slope & offset per channel
- issue: ceramic frames influence channels nearby
  - exclude channels from dE/dx measurement
- correct pad charge:

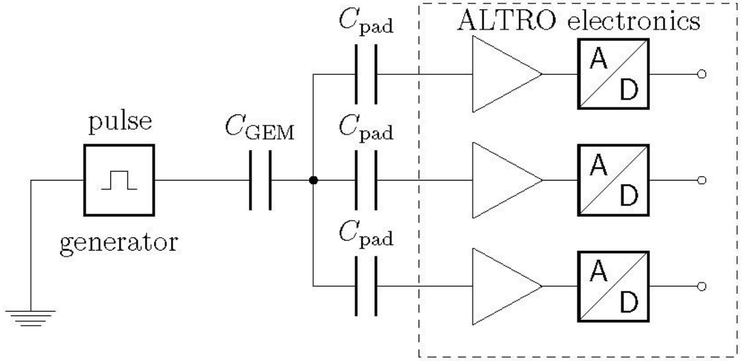


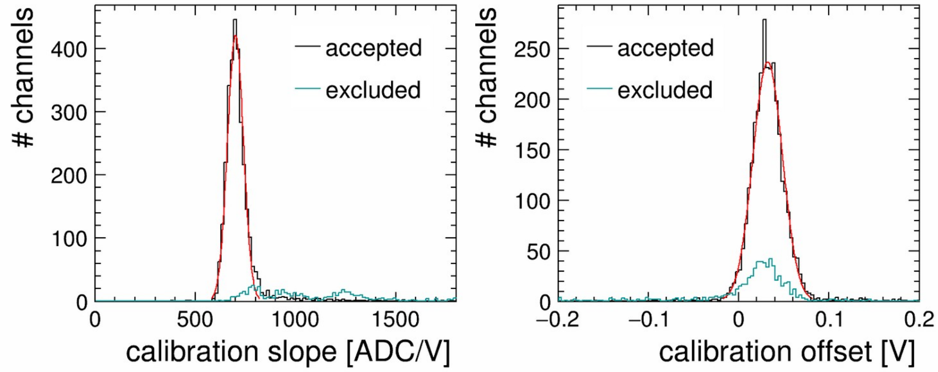

# Row Based Gain Correction

- normally: need correction for any location
  - requires 2D gain map
- test beam: track position is fixed in each run
  - intersect each pad row in one location
- calculate a correction factor for each row
- use average hit charge:
- calculated only on data subset

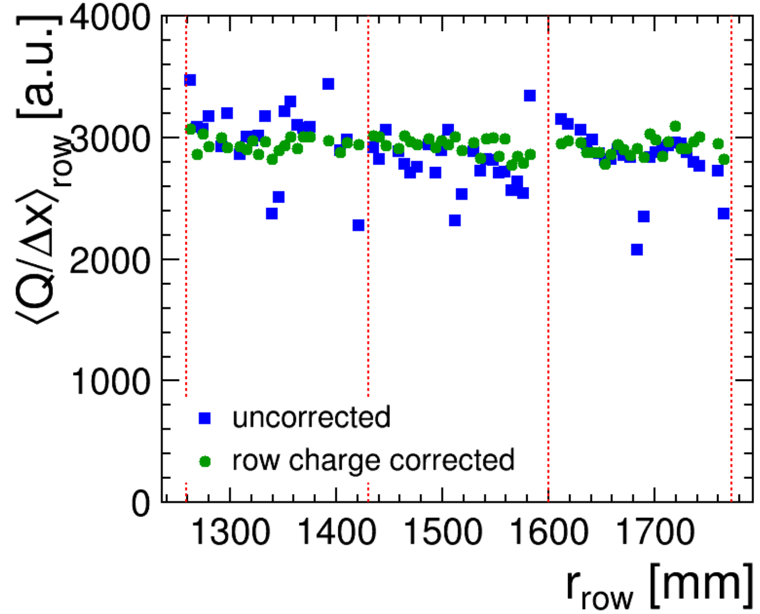

# Calibration Result

- test effect on dE/dx resolution
- process data with and without corrections
- no significant improvement
- expected: resolution dominated by primary ionisation
- larger fluctuations between runs

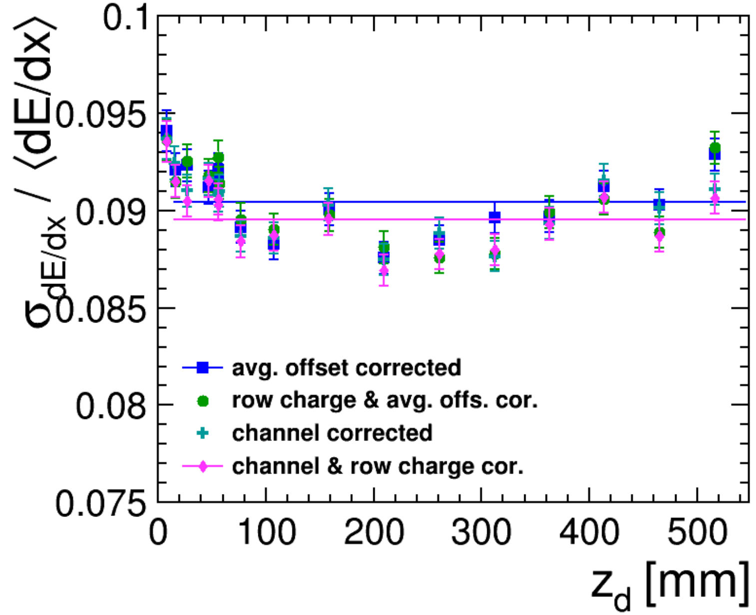

# Extrapolation to ILD

- extrapolate from LPTPC to ILD TPC
  - 56 hits to 220 hits
- dE/dx resolution scales with number of hits
  - power law $\sigma_0 \cdot N^{-k}, k < 0.5$
- idea: combine hits from multiple tracks
  → pseudo tracks of arbitrary length
- power law fit finds $k = 0.48$
- potential small bias due to method
- resolution at 220 hits (including bias): 4.8%
- fulfills ILD goal of 5 %

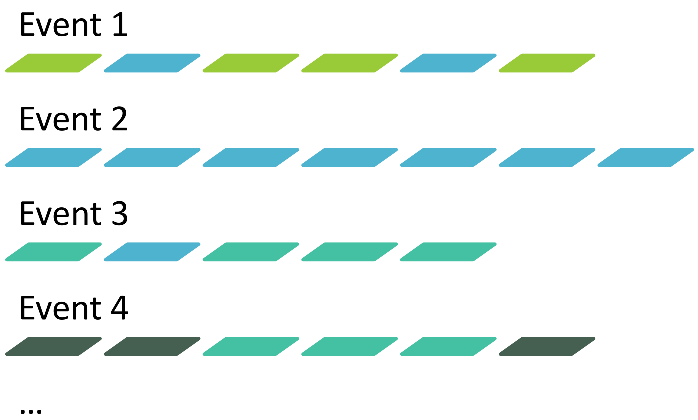

# Extrapolation to ILD

- extrapolate from LPTPC to ILD TPC
  - 56 hits to 220 hits
- dE/dx resolution scales with number of hits
  - power law $\sigma_0 \cdot N^{-k}, k < 0.5$
- idea: combine hits from multiple tracks
  → pseudo tracks of arbitrary length
- power law fit finds $k = 0.48$
- potential small bias due to method
- resolution at 220 hits (including bias): 4.8%
- fulfills ILD goal of 5 %